NASA Contractor Report 172351

NASA-CR-172351
19840011216

AN ANALYTICAL DESIGN PROCEDURE FOR THE DETERMINATION OF EFFECTIVE LEADING EDGE EXTENSIONS ON THICK DELTA WINGS

Farhad Ghaffari and Sushil K. Chaturvedi

OLD DOMINION UNIVERSITY RESEARCH FOUNDATION
Norfolk, Virginia

Contract NAS1-17099, Task 26
May 1984

National Aeronautics and
Space Administration

Langley Research Center
Hampton, Virginia 23665

ENTER:

```
     SELECT     TTL/AIME *+1 ANNUAL *+1    SE108: NEW USER SET NULL
     SELECT     TTL/AMERICAN INSTITUTE     SE104: TERM NOT IN DICTIONARY
 19      1      1 RN/NASA-CR-172351
          DISPLAY 19/2/1
      84N19284**   ISSUE 10   PAGE 1419   CATEGORY 2   RPT#: NASA-CR-172351 NAS
      1.26:172351   CNT#: NAS1-17099   84/05/00  80 PAGES   UNCLASSIFIED
      DOCUMENT
UTTL: An analytical design procedure for the determination of effective leading
      edge extensions on thick delta wings   TLSP: Final Report
AUTH: A/GHAFFARI, F.;  B/CHATURVEDI, S. K.
CORP: Old Dominion Univ., Norfolk, Va.   CSS: (Dept. of Mechanical Engineering
      and Mechanics.)    AVAIL.NTIS   SAP: HC A05/MF A01
MAJS: /*AERODYNAMIC COEFFICIENTS/*DELTA WINGS/*LEADING EDGES/*LIFT
MINS: / AIRCRAFT PERFORMANCE/ ASPECT RATIO/ SUPERSONIC AIRCRAFT
ABA:  Author
ABS:  An analytical design procedure for leading edge extensions (LEE) was
      developed for thick delta wings. This LEE device is designed to be mounted
      to a wing along the pseudo-stagnation stream surface associated with the
      attached flow design lift coefficient of greater than zero. The intended
      purpose of this device is to improve the aerodynamic performance of high
      subsonic and low supersonic aircraft at incidences above that of attached
      flow design lift coefficient, by using a vortex system emanating along the
      leading edges of the device. The low pressure associated with these
      vortices would act on the LEE upper surface and the forward facing area at
      the wing leading edges, providing an additional lift and effective leading
      edge thrust recovery. The first application of this technique was to a
ENTER:
```

SUMMARY

An analytical design procedure for Leading-Edge Extensions (LEE) has been developed for thick delta wings. This LEE device is designed to be mounted to a wing along the pseudo-stagnation stream surface associated with the attached flow design lift coefficient of greater than zero. The intended purpose of the device is to improve the aerodynamic performance of high subsonic and low supersonic aircraft at incidences above that of attached flow design lift coefficient, by using a vortex system emanating along the leading edges of the device. The low pressure associated with these vortices would act on the LEE upper surface and the forward facing area of the wing leading edges, providing an additional lift and effective leading edge thrust recovery.

The first application of this technique was to a thick, round-edged, twisted and cambered wing of approximately triangular planform having a sweep of 58° and aspect ratio of 2.3. The panel aerodynamics and vortex lattice method with suction analogy computer codes were employed to determine the pseudo-stagnation stream surface and an

optimized LEE planform shape, respectively.

The aerodynamic effectiveness of thirty six different LEE planform shapes were examined for the given wing by considering the influence of geometrical parameters such as chord, sweep angle and span extent. This investigation showed that the outboard reduction of the LEE span-extent minimizes the lift-to-drag ratio, regardless of the LEEs' planform-shape and area. Also, with the same planform area, it was found that constant chord is relatively more effective than LEEs having sweep angles less than that of the wing. Further, relative to the wing root chord and span, a 3.2% constant chord LEE with 89% span extent was selected as being the best candidate for the final design planform.

LIST OF SYMBOLS

A	aspect ratio, b^2/S_{ref}
b	span
C_D	drag coefficient, $drag/q_\infty S_{ref}$
C_L	lift coefficient, $lift/q_\infty S_{ref}$
C_m	pitching moment coefficient, $pitching\ moment/q_\infty S_{ref}\bar{c}$
C_p	pressure coefficient, $(p-p_\infty)/q_\infty$
ΔC_p	lifting pressure coefficient, $C_{p,l} - C_{p,u}$
$C_{p,l}$	lower surface pressure coefficient $(p_l - p_\infty)/q_\infty$
$C_{p,u}$	upper surface pressure coefficient $(p_u - p_\infty)/q_\infty$
C_s	leading-edge suction force
c	chord
$\bar{c}$	reference chord, mean aerodynamic chord
L/D	lift-to-drag ratio
M	Mach number
p	static pressure
q	dynamic pressure
S	wing projected area
V_x	x-component of the total velocity vector
V_y	y-component of the total velocity vector
V_z	z-component of the total velocity vector
x, y, z	coordinate axes centered at the leading edge apex
$\bar{x}/c$	fractional distance along the local chord of the wing or the pseudo-stagnation stream surface

SUBSCRIPTS

d	design
LEE	Leading-Edge Extension

SUBSCRIPTS (concluded)

l	lower
r	root
ref	reference
t	tip
u	upper
xx, yy, zz	second partial derivative with respect to x, y, z, respectively
o	value at $C_L = 0.0$
∞	free stream

GREEK SYMBOLS

α	angle of attack, degrees
η	fraction of wing semispan, η=1.0 is wing tip
η_{LEE}	b_{LEE}/b
Λ	leading edge sweep angle, degrees
ϕ	velocity potential

ABBREVIATIONS

FVS	Free Vortex Sheet
IC	Influence Coefficient
LEE	Leading Edge Extension
LEVF	Leading-Edge Vortex Flap
PSSS	Pseudo-Stagnation Stream Surface
PAN AIR	Panel Aerodynamics Computer Code
SA	Suction Analogy
SLEE	Sharp Leading Edge Extension
VLM	Vortex Lattice Method

Chapter 1

INTRODUCTION

Future high-subsonic or supersonic cruise swept wing aircraft are likely to be required to operate efficiently over an extended portion of their flight envelope. There are two basic approaches for designing such aircraft. The first, is a conventional approach, and seeks to maintain fully attached flow at each point of the envelope, whereas, the second approach attempts to use the organized separated flow at off-design and attached flow at design conditions. The design criterion of the conventional approach is more desirable, because an aerodynamically efficient aircraft always achieves its best performance with attached flow unless the wing is extremely slender. The primary cause of this high efficiency is the production of aerodynamic thrust associated with attached flow at the leading edge, as well as in the warped camber. The schematic flow representation of the techniques used to retain attached flow conditions at the leading edges of such swept wing aircraft are shown in Fig. 1.1. Variable camber at the leading edge, leading-edge flap, and large leading-edge radii are known for their potential to delay the onset of the leading-edge flow separation [1-3].* However, the

*The numbers in brackets indicate references.

natural tendency of flow towards separation for these wings, especially at off-design conditions such as for take-off, landing, and maneuvering, appears inevitable (see dash lines in Fig. 1.1). At off-design performance the flow characteristics of such aircraft are changed dramatically by the formation of a generally stable and coherent leading-edge vortex system. These vortices, which result from the leading-edge flow separation and subsequent flow reattachment on the remainder of the wing, are responsible for the changes which occur in the aircraft aerodynamic characteristics. For the purpose of illustration, Fig. 1.2 shows the typical flow types occurring over such aircraft at design and off-design conditions.

The resultant vortex system generates additional lift, caused by the low pressure regions under the stable vortex system, and produces the well known nonlinear aerodynamic behavior called "vortex lift." A typical comparison of the vortex lift, to that of attached flow lift is shown in Fig. 1.3. Accompanying the additional lift is the increased drag which results from the loss of the leading-edge suction associated with attached flow around the leading edge [4]. In addition to the drag penalty, the inboard movement of the center of the vortex coupled with the flow failing to reattach with increasing angle of attack, and vortex breakdown, results in a pitch-up condition [5]. These characteristics restrict high-g subsonic and transonic sustained maneuver, because of the excess engine thrust needed to overcome the drag-due-to-lift. As a result, the aerodynamic characteristics of the naturally occurring leading-edge flow separation over swept wing aircraft operating at off-

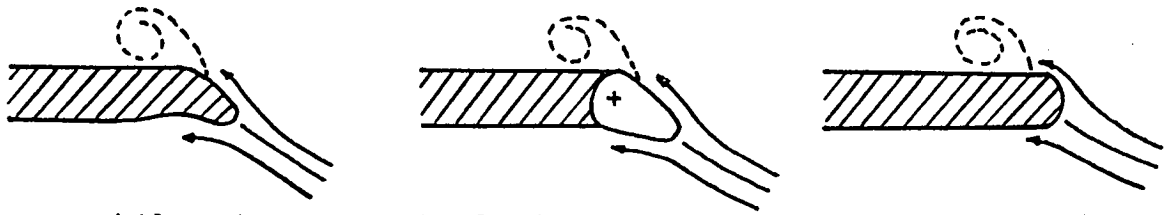

Fig. 1.1 Some techniques used at the leading edges of an aircraft to attain attached flow. (Streamwise cut)

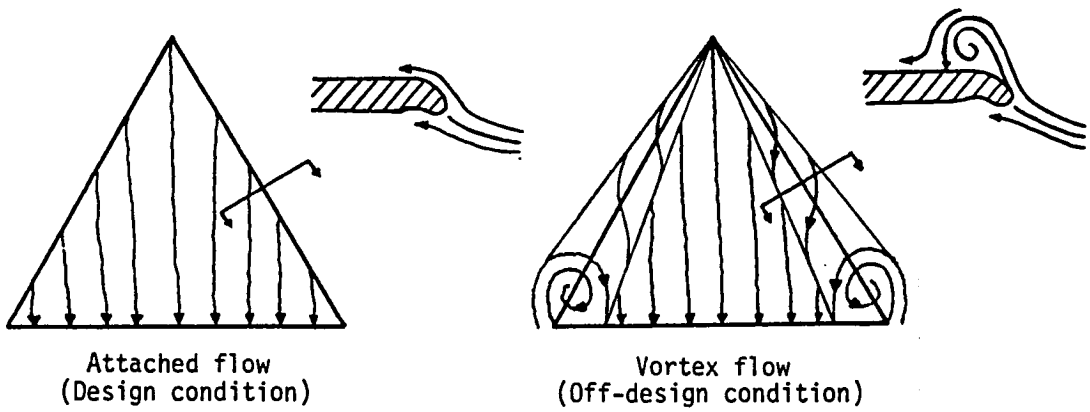

Fig. 1.2 Typical flow types occurring at the wing leading edges of an aircraft.

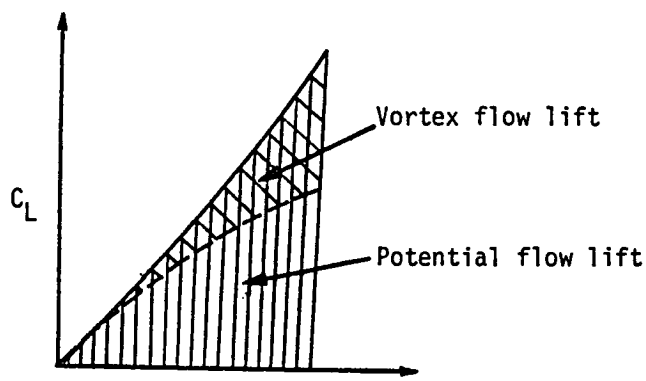

Fig. 1.3 Lift characteristics associated with attached and separated flow.

design conditions must be considered early in the aircraft design cycle.

As technology in aircraft design has developed, methods for improving multimission capability have been explored. One such method, the subject of this study, is to design the wing to achieve fully attached flow at the cruise design condition, and controlled leading-edge separation at take-off, landing, and maneuvering [3]. This method is an alternative approach to the conventional attached flow, for designing a high-subsonic or supersonic cruise swept wing aircraft. The basic concept of this approach is to let the flow separate and roll up into an organized leading-edge vortex system which is located appropriately. For this purpose, a family of vortex control devices such as fixed and movable leading-edge extensions has been developed. For example, the Sharp Leading-Edge Extension (SLEE) is a fixed leading edge extension composed of a flat or bent plate attached to the wing lower surface and been employed on swept wing models with round leading edges [6, 7]. An example of a movable leading-edge extension is the Leading-Edge Vortex Flap (LEVF). This leading-edge device can be rotated about its hinge-line and set at scheduled deflection angles which vary with angle of attack and Mach number [8, 9]. The flow mechanism associated with the leading edge for swept wing aircraft with SLEE and LEVF is shown schematically in Fig. 1.4. Unlike the conventional attached flow approach, SLEE and LEVF benefit from the natural tendency of flow separation at the leading edges. Such devices, when properly designed and positioned, can confine the entire leading-edge vortices to their upper surface and

provide flow reattachment on the wing along the device knee or hinge line. As a result, the aircraft not only produces additional lift, but it also generates a thrust force component, as the low pressure associated with the confined vortices acts on the neighboring surfaces. These leading-edge vortex control devices have been validated experimentally through extensive parametric studies on different wing models [5-10].

Following the latter approach (i.e., letting the flow separation occur), the present study attempts to develop a different expression of the fixed leading-edge extension device concept. The intended purpose of the device, designated as Leading-Edge Extension (LEE), is to improve the aerodynamic performance of high-subsonic and low supersonic aircraft away from the conditions for cruise in general called off-design. The scope of the present study will be discussed subsequently in this chapter.

Pursuing the concept of leading-edge vortex control, a literature survey was conducted for devices that had potential for controlling the leading-edge flow separation of wings with moderate-to-highly sweptback leading edges. The next section presents an overview discussion on the aerodynamic effectiveness of devices such as SLEE and LEVF.

1.1 Literature Survey

In recent years, leading-edge extension devices have been the subject of extensive studies for improving the aerodynamic and pitching moment characteristics of high-subsonic and transonic aircraft, capable of maneuvering efficiently at high lift. One of the earliest efforts

made in using a leading-edge device was by Wilson and Lovell [10]. The objective of their study was to increase the $C_{L,max}$ of a 15% thick, blunt leading edge of an approximately 60° delta wing, designated as DM-1, by producing vortex flow over its upper surface. They determined experimentally that the flow separation required could be best achieved by employing a fixed part-span leading-edge extension on the vehicle. (The vehicle had a symmetrical airfoil and no twist so the design lift coefficient ($C_{L,d}$) was zero). As a result, their wind tunnel studies indicated that, attachment of this device increased the original $C_{L,max}$ of the DM-1 from 0.6 to 1.01 with essentially no drag penalty at low lift coefficients, only a slight increase at moderate C_L values, and a significant drag reduction at lift coefficient beyond 0.75. This initial study enlightened the importance of a leading-edge flow control device in the aerodynamic performance of an aircraft.

A series of different SLEE and LEVF devices have been investigated by Johnson and Rao [6] and Tingas and Rao [7] on a 60° swept, cropped-delta wing with round leading-edges. These experimental studies have shown a substantial improvement in drag reduction potential of both devices at moderate-to-high angles of attack. These authors have concluded that there is a need for a concerted effort to optimize the effectiveness of these devices, which function by maintaining the vortex on the upper surface of device, flow reattachment where the device joins the wing and attached flow on the rest of the wing. These studies further identify the following methods as having significant potential to increase the aerodynamic efficiency of such devices. They are:

tapering, twisting, segmenting, and proper mounting position on the wing.

Additional details concerning leading-edge flow control devices can be obtained from recent publications by Lamar and Campbell [11], and Rao [12].

1.2 Present Study

The objective of this study is to develop an extension to the device used by Wilson and Lovell, which would improve the aerodynamic performance and pitching moment characteristics of cambered and twisted high-subsonic and low-supersonic aircraft at off-design conditions. This leading-edge device, designated as a Leading-Edge Extension (LEE), is to be mounted to a wing along the Pseudo-Stagnation Stream Surface (PSSS) associated with the attached flow design lift coefficient ($C_{L,d}$) of greater than zero [11]. The PSSS is a dividing stream surface which separates the incoming flow into two regimes, in general over the upper and under the lower wing surface. Two streamwise cuts through the PSSS are shown schematically in Fig. 1.5 to illustrate the surface curvature. The present study seeks to determine a representation of the PSSS based on the following four assumptions. 1) There exists a PSSS associated with a swept wing aircraft at attached flow design condition. 2) The intersection of the PSSS with a number of parallel xz planes spanning the wing produces curves. 3) These curves can be represented by the pseudo-stagnation streamline leading to the pseudo-stagnation points and derived from the local slopes of the resultant velocities ($\sqrt{V_x^2 + V_z^2}$)

Fig. 1.4 Schematic mechanism of leading-edge flows over a wing with SLEE and LEVF. (Streamwise cut)

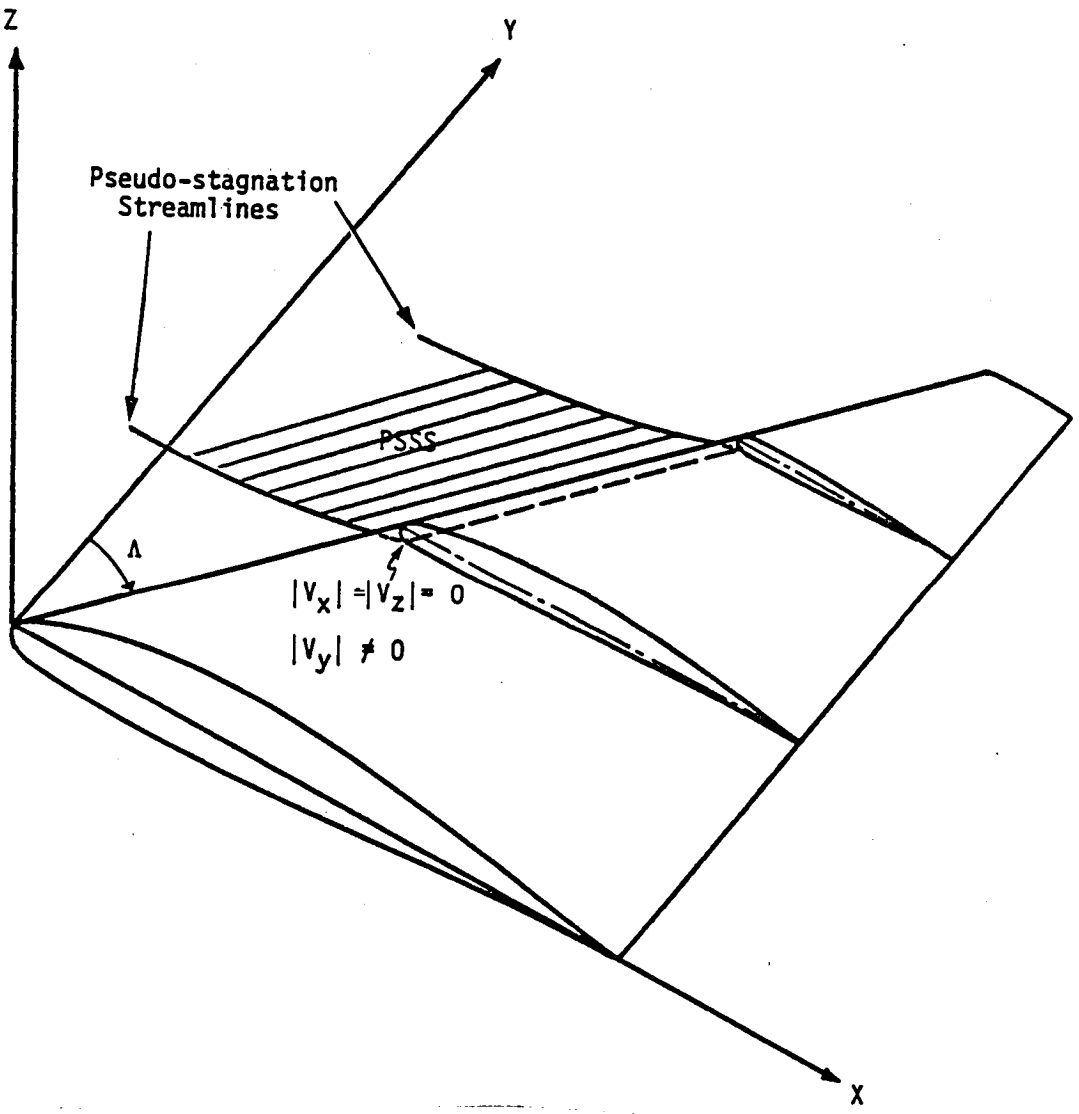

Fig. 1.5 Schematic representation of the PSSS corresponding to two airfoil sections of a wing.

at appropriate points in the xz plane. 4) A spanwise surface fitted linearly through the resulting intersections is an approximation of the PSSS described in assumption (1).

In order to accomplish the task of designing an aerodynamically efficient LEE planform shape, an analytical procedure had to be developed. This procedure which forms the basis of the present study can be outlined into two major steps:

a) Analytical determination of the PSSS at attached flow design condition for the wing.

b) Analytical optimization of the chordwise extent and the planform shape of the PSSS at separated flow conditions. This step would in fact determine the optimum LEE size for the given wing.

To demonstrate the procedure outlined above, a candidate wing and computer codes (i.e., analytical tools) had to be selected. As a result, a thick, round-edged, twisted and cambered wing of approximately triangular planform having a sweep of 58° and aspect ratio of 2.3, was chosen to provide the first application of this technique. The planform view of this wing model is shown in Fig. 1.6. At the outset, four computer codes were considered to be the options for analytical execution of the present study at a high subsonic Mach number. These codes were Free Vortex Sheet (FVS), Panel Aerodynamics (PAN AIR), Vortex Lattice Method with Suction Analogy (VLM-SA) [13-15], and a transonic computer code. Although, attempts were made to obtain and employ a transonic computer code in this study, due to the high subsonic Mach

numbers of interest, none was available when this study began which could reliably estimate the pressures on thick-delta wings. Following elimination of this code, the FVS was also excluded from the code options because of the authors' unsuccessful past experience which included efforts to obtain a converged solution for the DM-1 + LEE combination of Reference 10. Hence, the available computer code options were reduced to two, namely PAN AIR and VLM-SA codes. Further, after unsuccessful attempts for determining the velocity field solutions by VLM-SA because of the thickness omission by the code, the PAN AIR code was assigned to perform the task. The task was successfully accomplished and the velocity field solutions for different wing sections were analytically determined at the attached flow design lift coefficient ($C_{L,d}$) of 0.25 and Mach number of 0.8. (Note that this value of $C_{L,d}$ was used to simulate the design angle of attack (α_d) of 6.0°). Neglecting the sidewash (V_y) effect, the resultant velocity vectors obtained from vectorial addition of the axial (V_x) and the upwash (V_z) velocity components associated with each wing section were plotted, and the corresponding pseudo-stagnation streamlines were graphically determined. The resulting stagnation streamlines were designated as being "pseudo" because they did not correspond to the actual stagnation point where the magnitude of the three velocity components are all zero. In fact, except at the center line of a three-dimensional swept wing there exists no other point on the wing surface, from a potential flow viewpoint, where zero sidewash velocity will occur. As a result, the pseudo-stagnation streamline solutions correspond to certain points on the wing

surface where only the magnitude of V_x and V_z components of the total velocity are zero. Consequently, the determined pseudo-stagnation streamlines, are the planar cuts through a surface which represent the "pseudo" stagnation stream surface. Lastly, a portion of the determined PSSS solution is to be designated as the shape of the LEE device.

The LEE acts as a dividing stream surface. In general, depending upon the accuracy with which the LEE (or the PSSS) is determined, its presence, other than a small skin friction drag, should not affect the main wing aerodynamic performance at the designed angle of attack (α_d) of 6.0° (see Fig. 1.7a). However, at higher angles of incidence, vortices would be generated as a result of forced flow separation by the sharp leading edges of the LEE device. These vortices can be controlled through LEE planform shape optimization by varying parameters such as the chordwise extension, spanwise extension, and leading-edge sweep angle. As shown in Fig. 1.7b, a properly designed LEE planform, can capture the entire leading-edge vortices on its upper surface and provide flow reattachment at, or near the wing upper surface leading edge. The confined leading-edge vortex system induces suction pressure which acts on the LEE surface and the forward-facing area of the wing leading edges, providing an additional lift and an effective leading-edge thrust recovery. As a result, the aerodynamic thrust force generated in the flight direction yields a reduction in drag, relative to a planar configuration, and the added lift permits the aircraft to operate at lower angles of attack which may delay the pitch-up moment problem.

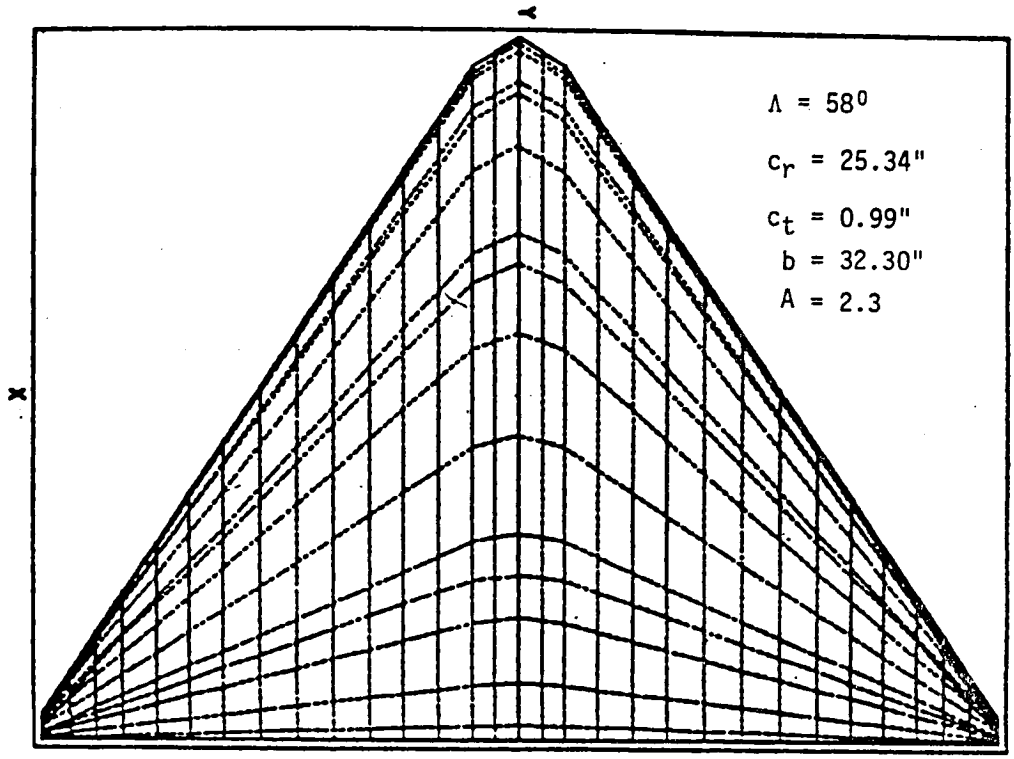

Fig. 1.6 Planform of the wing model.

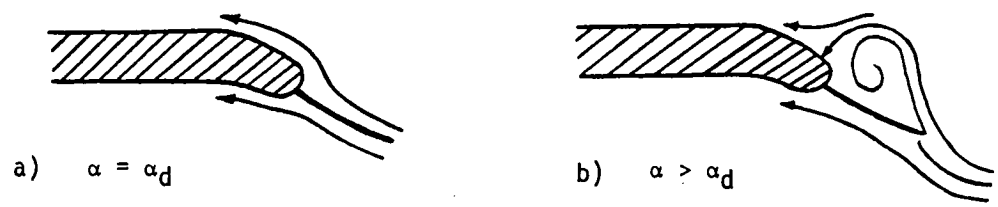

Fig. 1.7 Leading edge flow mechanism of a wing-LEE combination at a) design angle of attack, b) off-design angle of attack. (Streamwise cut)

Chapter 2

DETERMINATION OF PSEUDO-STAGNATION STREAM SURFACE (PSSS)

This chapter discusses in detail the application of the PAN AIR code and the procedure employed for determining the PSSS of the wing model at the attached flow design condition. Further, Appendix A provides a brief discussion on the PAN AIR code and a test which was conducted for validating the resulting PSSS solution.

2.1 Method Employed

PAN AIR code is a system of computer programs for the detailed analysis and the non-iterative design of arbitrary aircraft configurations in three-dimensional, steady, inviscid, irrotational, subsonic and supersonic flows. The configuration surface is partitioned into several "networks," each approximated by a set of panels on which unknown source and doublet singularity distributions are assigned. By imposing boundary conditions at a discrete set of points, the integral equation solution to the partial differential equation is reduced to a system of linear algebraic equations relating the unknown singularity strengths which in turn determine the properties of the flow field. Additional discussion on some of the capabilities and limitations of the PAN AIR code are explored in Appendix A.1.

The PAN AIR computer code was employed in the present study to determine the velocity field solution of the wing model at the attached

flow design angle of attack (α_d) of 6.0° and Mach number of 0.8. For this purpose, the survey network coupled with the Influence Coefficient (IC) update capability (see Appendix A.1) of the code was first exercised. Several attempts were made, but due to the problems introduced by the IC-update package, efforts to use this economically efficient approach had to be terminated. As a result, only the survey network capability of the code was employed in the present study to determine the velocity field solution of the wing model at the design condition. This task was successfully accomplished using the PAN AIR code and resulted in graphical determination of the PSSS for the wing model. Sections 2.2 and 2.3 discuss the procedure involved in determining the PSSS.

2.2 Survey Networks

The survey networks adopted in the present study were vertical xz planes located at sixteen different stations along the semi-span of the wing model. These survey networks were generated such that, each would enclose the nose portion of its corresponding station and stand-off from the section a distance of approximately equal to .08% of the wing c_r. The networks began at the upper surface just behind the leading edge and extended around the nose to the lower surface mid-chord. Due to the similarity of the survey network geometries and the involved process of their generation, only a typical survey network (located at the fourth station) shown in Fig. 2.1, will be discussed. This figure also shows the planform distribution of the other survey network locations over the

semi-span of the wing model. Further, the enlarged cross sectional view of the survey network and the nose portion of its corresponding airfoil section at the fourth station is shown in Fig. 2.2a. Since the PAN AIR Code velocity field solutions were assigned to be calculated at the center point of each panel in a particular survey network, it was essential to provide the survey networks with enough panels, so that, once the resultant velocity vectors, associated with V_x and V_z, were plotted, the pseudo-stagnation streamlines could be depicted graphically for each wing section. For this purpose, a geometrical computer code, called GEOMABS [16], was employed to intensify the paneling on the survey networks. Figure 2.2b, shows the repaneled survey network. It can be seen from the figure that the panel density is concentrated primarily around the portion of the survey network which faces the nose of the associated wing section. This would provide more velocity vector solutions needed to determine graphically the accurate location of the resulting pseudo-stagnation streamlines, as they meet their corresponding wing section. Similar survey networks were generated for all sixteen semi-span stations of the wing model. Each individual survey network was positioned on the wing model and a separate PAN AIR code execution was performed.

2.3 Flow Field and the PSSS Solution

The PAN AIR code executions yielded the axial (V_x), the sidewash (V_y), and the upwash (V_z) velocity components at the panels center points of each survey network. The resultant velocity vectors, obtained

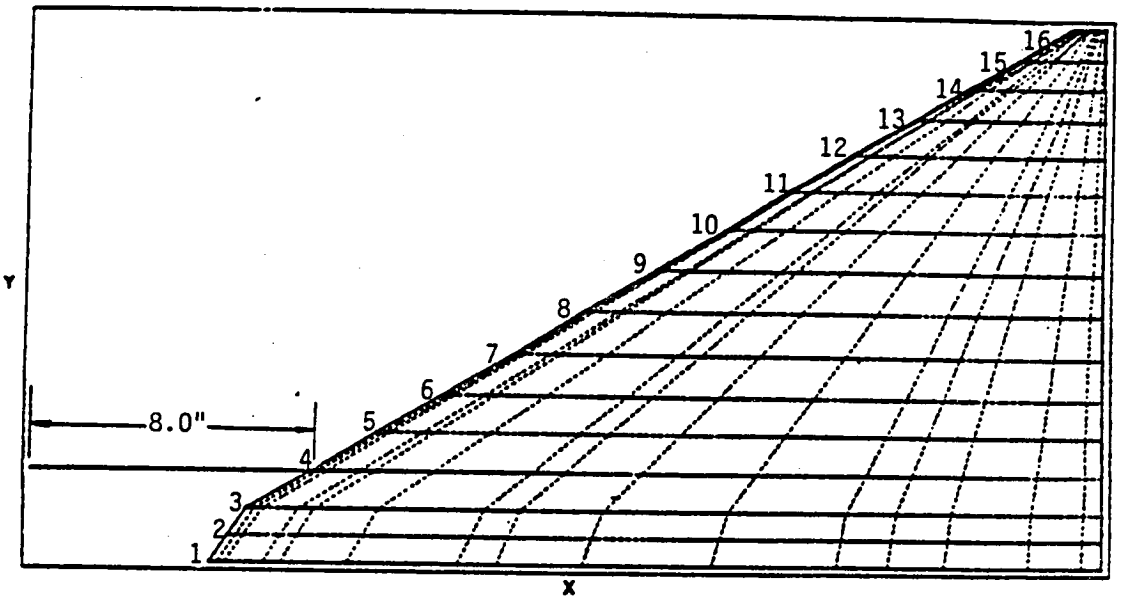

Fig. 2.1 Semi-span planform view of the wing model with a survey network located at fourth station.

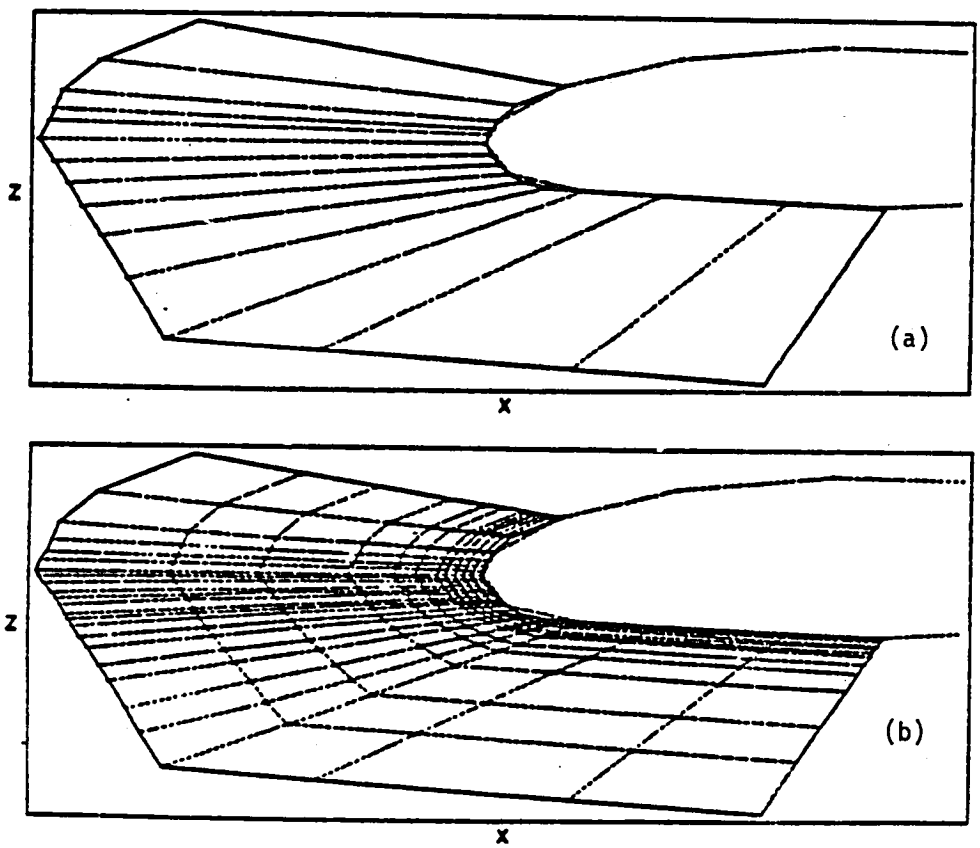

Fig. 2.2 Enlarged cross-sectional view at fourth station.
a) original panels.
b) densed-up panels.

from the vectorial addition of the axial and the upwash velocity components were plotted at the center point of each panel for a given survey network. An example of these plots is shown in Fig. 2.3a. For a given survey network, the streamline associated with minimum velocity magnitude (i.e., $|V_x| \approx |V_z| \approx 0$, pseudo-stagnation point) was drawn tangent to the plotted velocity vectors. As mentioned earlier, these streamlines were designated as pseudo-stagnation streamlines. Fig. 2.3b shows the nose portion of an airfoil section with its corresponding velocity field and the graphical pseudo-stagnation streamline solution. These graphical streamline solutions yielded their coordinate points relative to the corresponding wing section. A cubic spline curve was fitted through the graphically determined coordinate points, associated with each pseudo-stagnation streamline, to ensure the smoothness of the resulting streamline solutions. Each of these solutions were equally extended out a distance of 4.8" (i.e., 19% of the wing c_r) ahead of the wing leading edge. This distance was thought to be sufficient for the present analysis of the LEE device.

The unrealistic velocity field solutions obtained at the tip region prevented the graphical generation of the pseudo-stagnation streamlines for the last two wing sections because of the manner in which the tip thickness was modeled.† As a result, this unrealistic solution at the tip section affected the flow field of the neighboring station as well

†It was subsequently learned that unrealistic flow field solutions could be expected to occur in the tip region, if the wing thickness there was zero (private communication with Larry L. Erickson of NASA Ames). It is anticipated that this problem will be reexamined in the near future, so that the remaining pseudo-stagnation streamline solutions, at the tip region, would be determined.

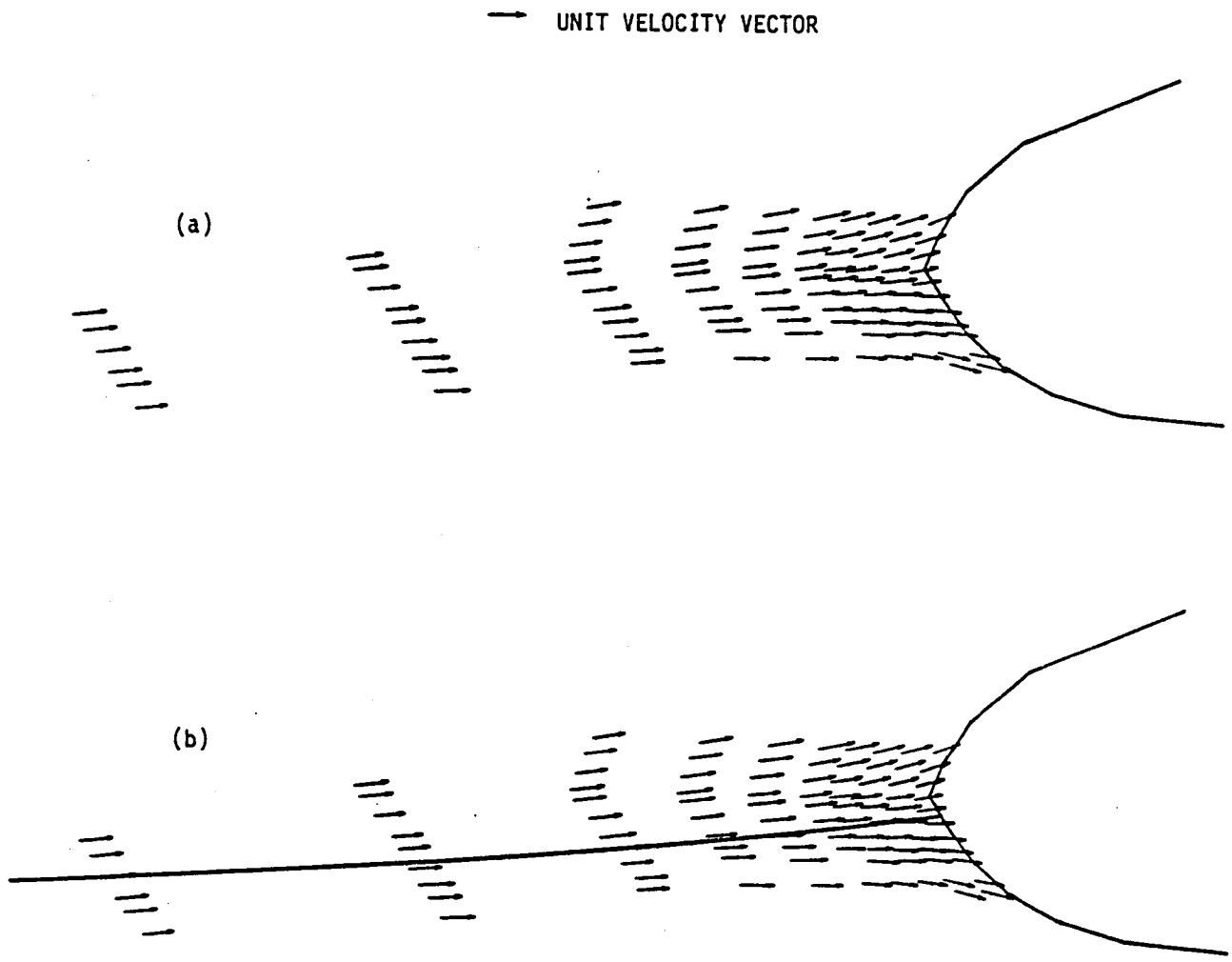

Fig. 2.3 Fourth station, a) velocity field solution, b) pseudo-stagnation streamline solution.

tip section affected the flow field of the neighboring station as well (i.e., 15th station).

A warped surface was linearly fitted spanwise through the available pseudo-stagnation streamline solutions and was designated as the PSSS. The three views of the determined PSSS solution are shown in Fig. 2.4. Further, five sectional cuts through the wing-PSSS combination and the enlarged cross sectional view of the same cuts are shown in Fig. 2.5. Approximately the resulting PSSS has a semi-span of 14.33" (i.e., 89% of the wing semi-span) and a constant chord of 4.8".

It was essential to examine the degree of accuracy of the determined PSSS solution. For this purpose, the PAN AIR code was employed once again to model the wing-PSSS combination at the design condition by specifying the PSSS as being a lifting surface. This investigation is discussed in detail in Appendix A.2. From this pressure distribution study, it was concluded that the resulting PSSS solution is a good approximation of the actual dividing stream surface associated with the wing model at the attached flow design condition.

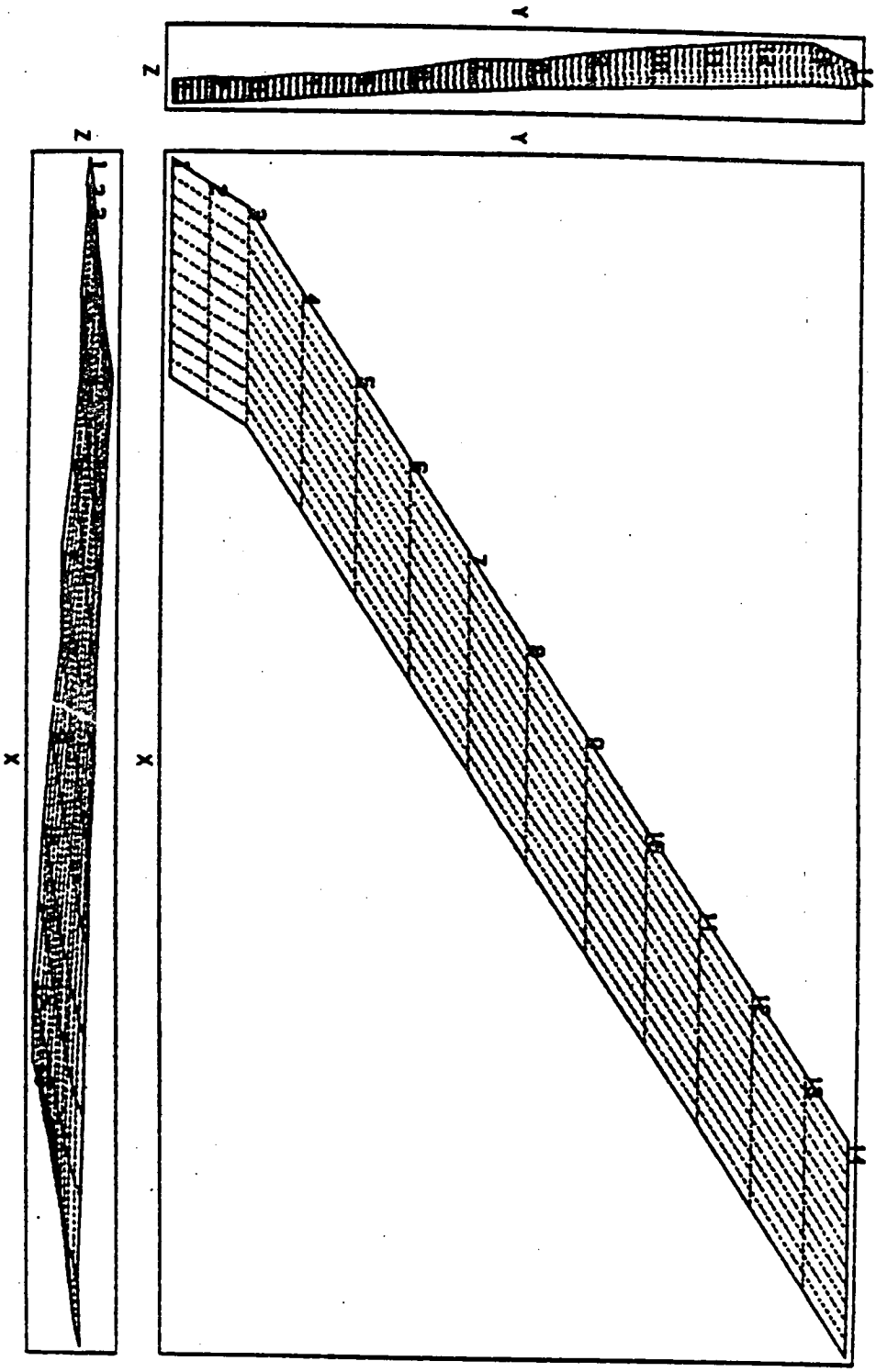

Fig. 2.4 Three views of the determined PSSS solution.

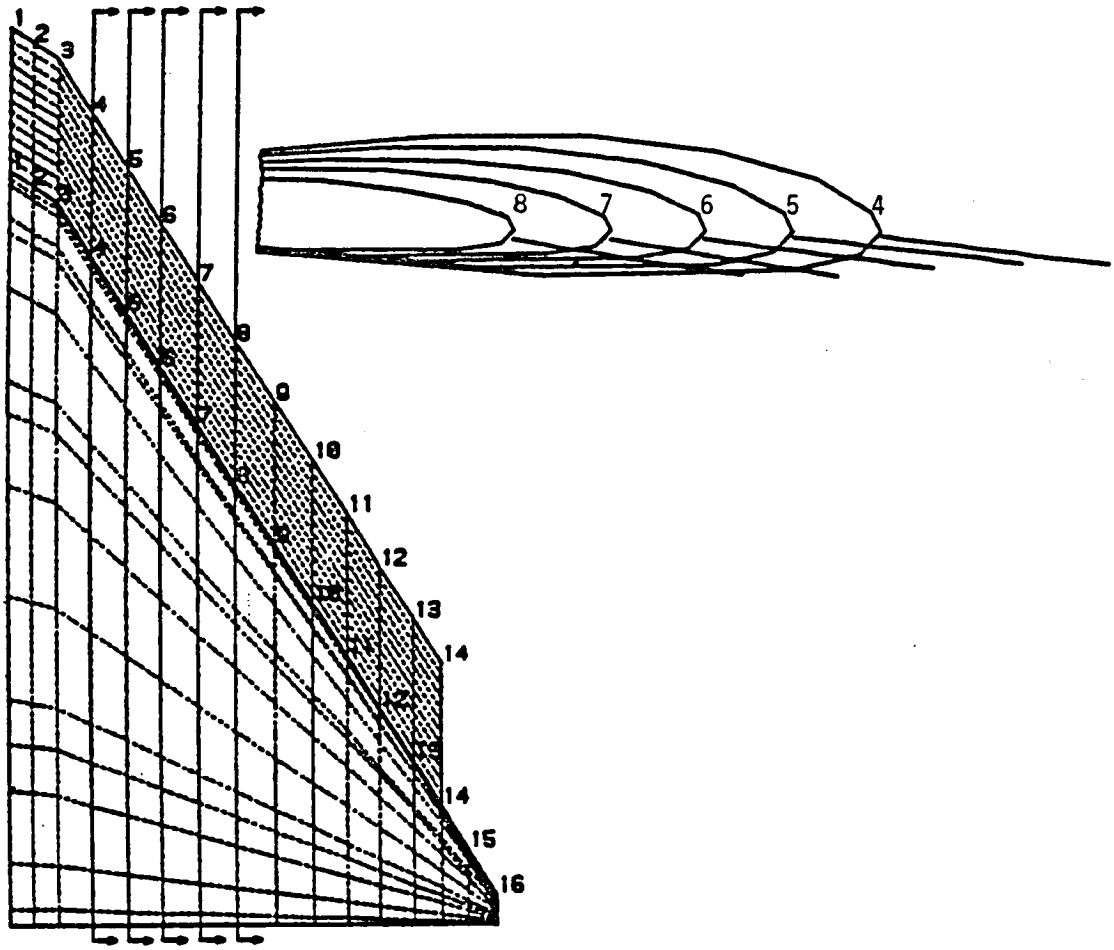

Fig. 2.5 Sectional cuts through the wing-PSSS combination and enlarged cross sectional views.

Chapter 3

RESULTING LEADING-EDGE EXTENSION (LEE) EFFECTS

This chapter discusses in detail the application of the VLM-SA code in the present study for determining an effective LEE planform shape for the wing model. A brief discussion on some of the code capabilities and limitations is presented in Sec. 3.1, and these have been further expanded in Appendix B. The effect of various LEE constant chord, span, and sweep angle are discussed in Secs. 3.2-3.4, respectively.

3.1 Method Employed

Vortex Lattice Method coupled with Suction Analogy (VLM-SA) developed at NASA Langley Research Center estimates overall forces and moments of complex planforms at subsonic speeds. The code is based on steady, inviscid, irrotational, incompressible flows, and uses the Prandtl-Glauert rule to account for compressibility. It approximates the continuous distribution of bound vortices over a lifting surface by a finite number of elemental panels which are then replaced by horseshoe vortices. The resultant force contribution of an individual panel is determined by imposing the no-flow penetration boundary condition to each of the elemental panels. These forces are then summed appropriately to obtain lift, drag, thrust and pitching moment. Additional discussion on VLM-SA code is presented in Appendix B.1.

The VLM-SA code is employed in the present study to investigate the

effects of the presence of the LEE device, as well as its geometrical parameter variation, on the aerodynamic characteristics of the thick, twisted and cambered, basic wing model. Although the twist and camber of the wing model is represented by its mean camber surface, the thickness effect is ignored by the VLM-SA code (see Appendix B.1). A computer program was developed to generate the required slopes at the control point (also called the local angle of attack) of each elemental panel located along the mean camber surface of the wing model. This program was further modified and used to find the local angles of attack for the warped surface of the LEE device. These two programs are listed in Appendix B.2. In addition, an effort has been made to evaluate the capability of the VLM-SA code in predicting the total aerodynamic vortex-induced forces for a wing-LEE configuration, similar to the one employed in the present study. This discussion is presented in Appendix B.3.

The analytical solutions for the basic wing model of the present study were first intended to provide a base line for comparative assessments of the LEE device. However, as discussed in Appendix B.3, this approach appears unjustified, because it is suspected that the VLM-SA would estimate the drag pessimistically in the case of wing-LEE analysis of the present study. As a result, throughout this study the aerodynamic effectiveness of different wing-LEE combinations will be emphasized relative to one another rather than to the basic wing model.

3.2 Constant Chord

Analytical estimates of the total vortex-induced forces and moments

were generated on the wing model as well as with selected constant chord LEE configurations by employing the VLM-SA code. There were a total of six constant chord LEEs examined in this study. The selected chord dimensions included 4.8", 3.6", 2.4", 1.6", 1.2", and 0.8". All these examined LEEs had a semi-span of 14.33". The planform view of the wing model with these LEEs are schematically shown in Fig. 3.1. The code estimates were generated using seven chordwise and 25 spanwise horseshoe vortices on the half-span of the wing model, and another 7-by-21 array of horseshoe vortices were used on the LEE planforms.

The VLM-SA code estimates of drag and lift coefficients for the basic wing as well as for the wing-LEE configurations are plotted in a drag polar form in Fig. 3.2. Although, the solutions include the aerodynamic performance of wing-LEE combinations below $C_{L,d}$ (i.e., 0.25), it is practical only to examine their aerodynamic effectiveness at higher lift coefficients. As shown in the figure, at the design lift coefficient, the attachment of the LEE device produces only a slight additional drag as compared to the basic wing, regardless of the LEE planform area. As was verified by PAN AIR code (Appendix A.2), these results also indicate that the LEE (PSSS) devices are good representations of the dividing stream surface associated with the wing model at the attached flow $C_{L,d}$. These results are remarkable considering the differences between the theoretical methods employed by each code.

The drag polar comparison reveals that 0.8" and 1.2" constant chord LEEs produce nearly the same aerodynamic effectiveness through lift coefficient range of about 0.25 to 1.20. However, it appears that consid-

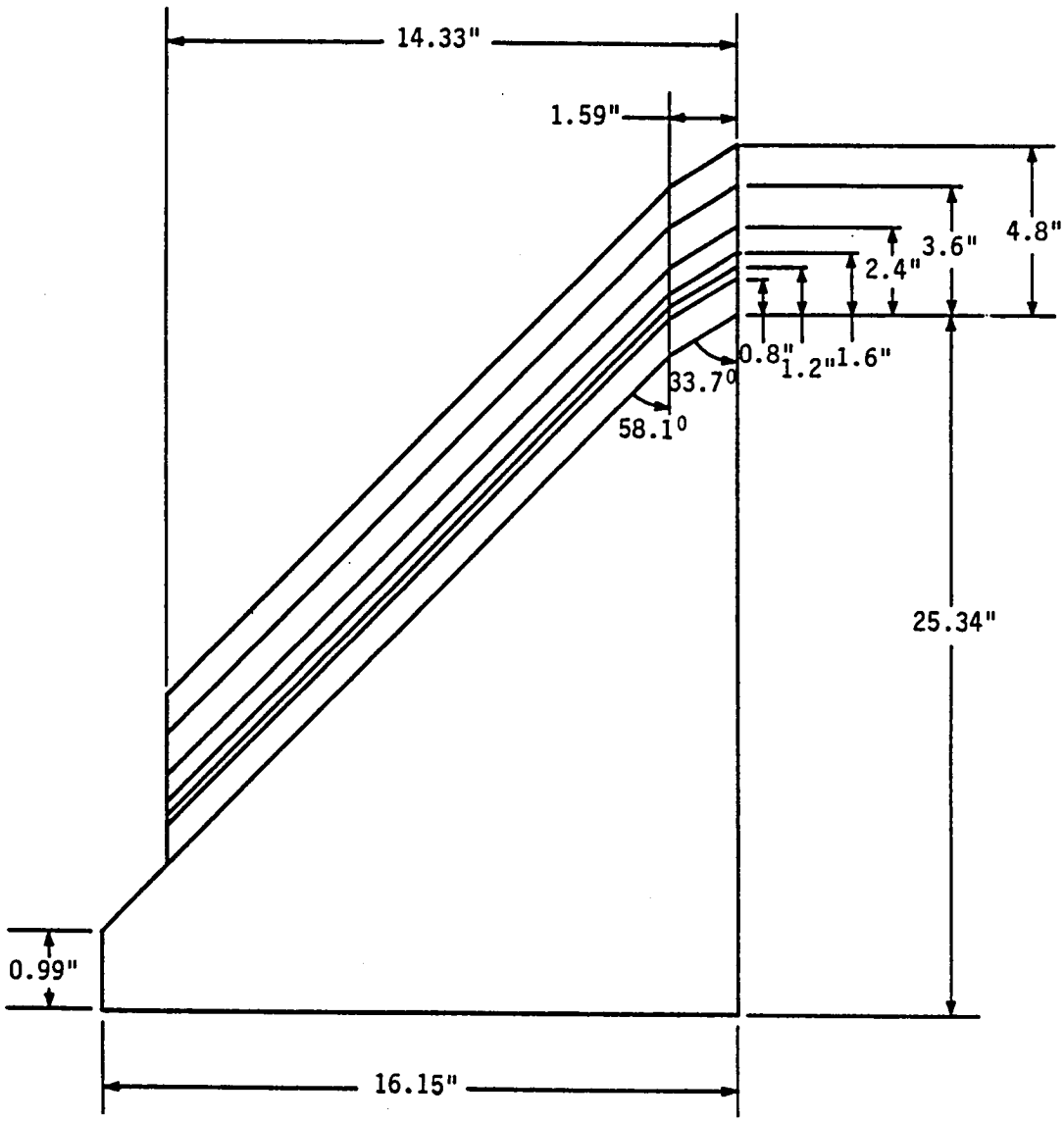

Fig. 3.1 Schematic planform view of the wing model and the selected constant chord LEEs.

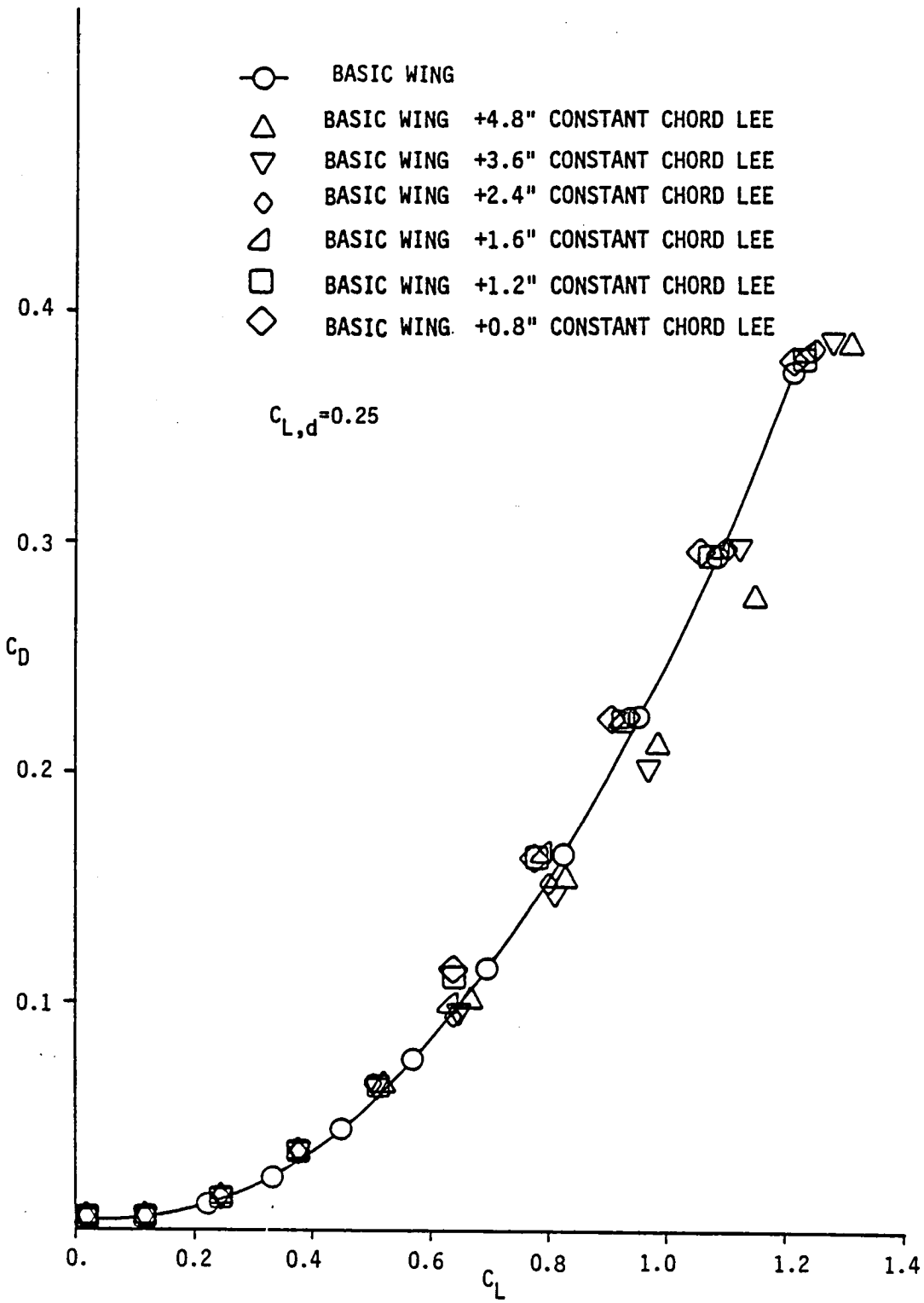

Fig. 3.2 Effect of constant chord length for LEE on drag polar, η_{LEE}= 89%.

erable improvement can be achieved in the lift and drag characteristics of the wing-LEE combination by employing a longer LEE chord extension. For example, as compared to 1.2" and 0.8", 2.4" constant chord LEE produces less drag in the lift coefficient range of 0.50 to 1.20. Also, this figure shows for the same lift coefficient range, 4.8" constant chord LEE has a remarkable drag reduction capability. In fact, it produces minimum drag beyond the lift coefficient of 1.0. Further, the same results are shown in Fig. 3.3, where lift-to-drag ratio is plotted against lift coefficient. This figure also indicates that, a 4.8" constant chord LEE achieves the best aerodynamic performance throughout the lift coefficients beyond $C_{L,d}$. However, from the practical point of view it should be mentioned that the final LEE planform design should have a chord dimension which is relatively shorter than the wing local chord, especially in the tip region. A smaller chord LEE not only benefits from the reduced structural weight, but it also minimizes the effect of bending moment about the wing-LEE junction. This bending moment occurs at off-design performances as the low pressure associated with the leading-edge vortices act on the upper surface of the LEE device. As a result, the present study seeks to design a LEE which employs both minimum area and chord. These two design criterion are referred to as the design requirements of the present study.

3.3 Sweep Angle

The aerodynamic effects of six different LEE sweep angles (Λ_{LEE}) were investigated in the present study by employing the VLM-SA code.

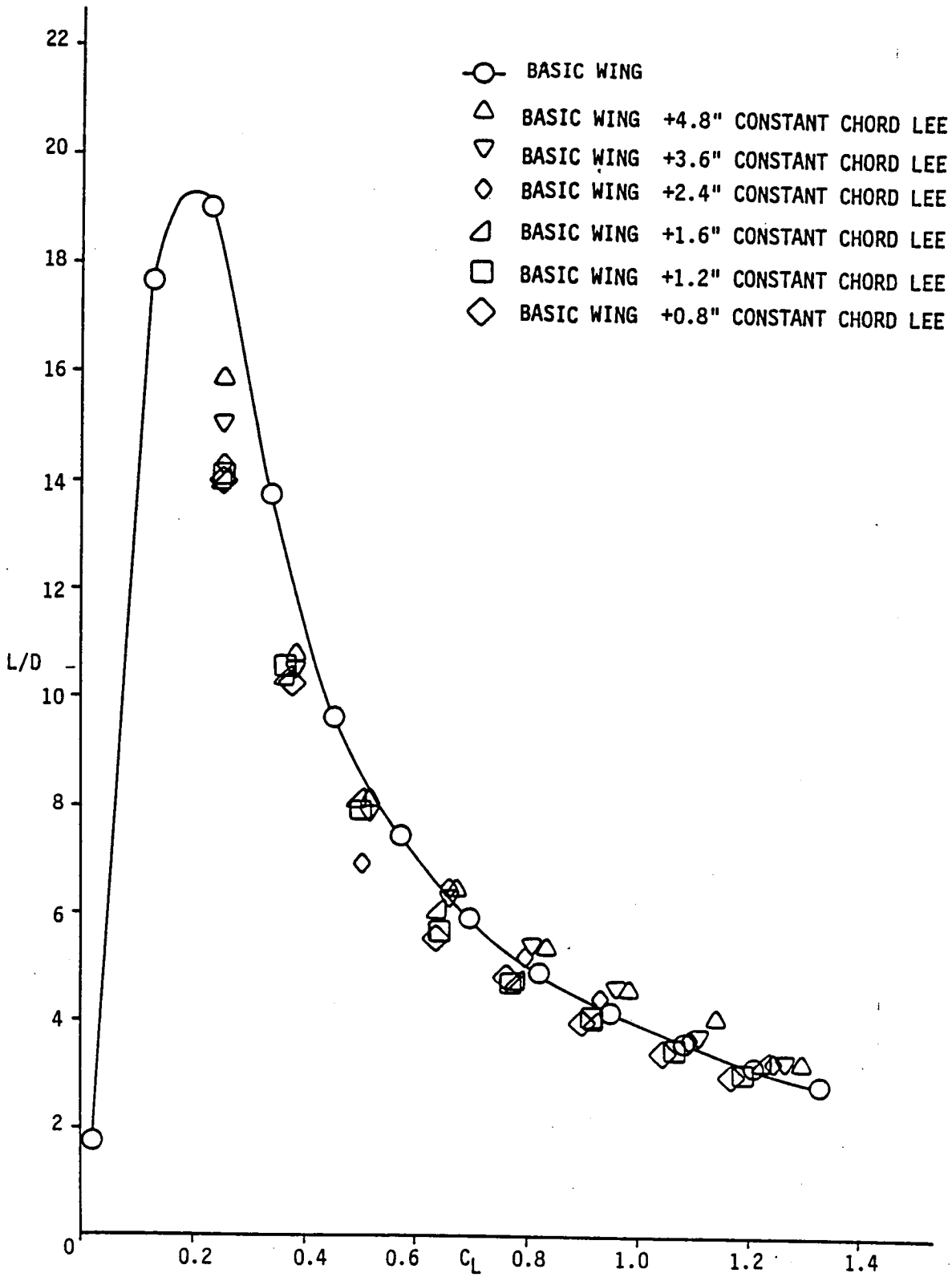

Fig. 3.3 Effect of constant chord length for LEE on lift-to-drag ratio, η_{LEE}=89%.

A schematic planform view of the wing model and the LEE sweep angles are shown in Fig. 3.4. The selected angles include 53°, 54°, 55°, 56°, 57°, and 58°. These angles are measured from a horizontal line which passes through a point located at a distance of 0.8" ahead of wing leading edge along the pseudo-stagnation streamline associated with the third semi-span station. All the selected LEEs had a semispan of 14.33" which is equal to 89% that of the wing model. Figure 3.4 also shows the LEE's tip chord dimensions. The VLM-SA estimates were obtained by using the same number of horseshoe vortices on the wing and the LEE planforms as were used in the previous section.

The resulting VLM-SA solutions of lift and drag coefficients are shown in Fig. 3.5. This figure shows that, except in the lift coefficient range of about 0.6 to 1.0, Λ_{LEE} variation has only a slight effect on the drag and lift characteristics of the wing-LEE configuration. This is an interesting result. As shown in Fig. 3.4, the LEE area and the corresponding tip chord decreases as Λ_{LEE} increases. In fact, 53° sweep angle LEE has twice the area as 57° sweep angle, however, they both produce almost the same drag characteristics at low and high lift coefficients. At moderate lift coefficients (0.6 to 1.0), it appears that LEEs with lower sweep angle are more effective in reducing the drag. The same conclusion can be derived from Fig. 3.6, where lift-to-drag ratio is examined at different lift coefficients.

It appears instructive to compare the aerodynamic effectiveness of different LEEs relative to their planform area by considering the effect

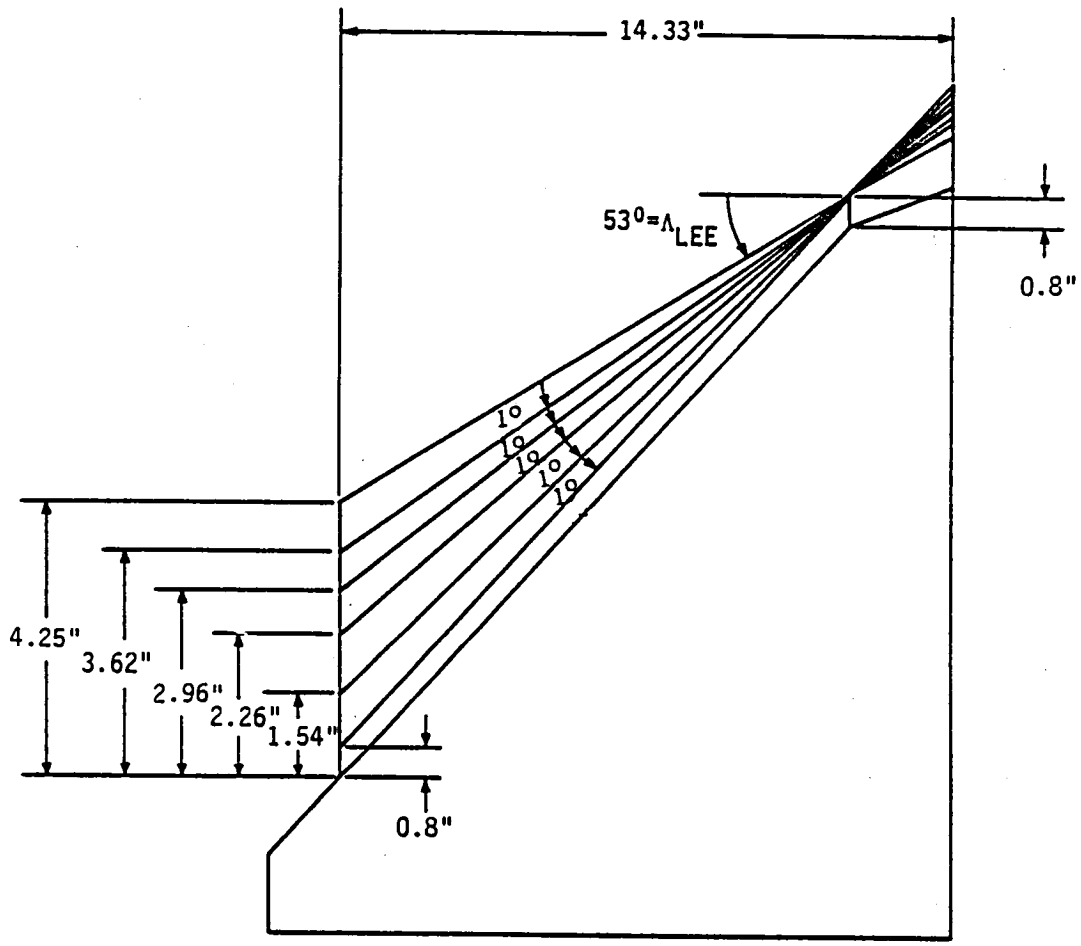

Fig. 3.4 Schematic planform view of the wing model and the selected LEEs with different sweep angles, η_{LEE}=89%.

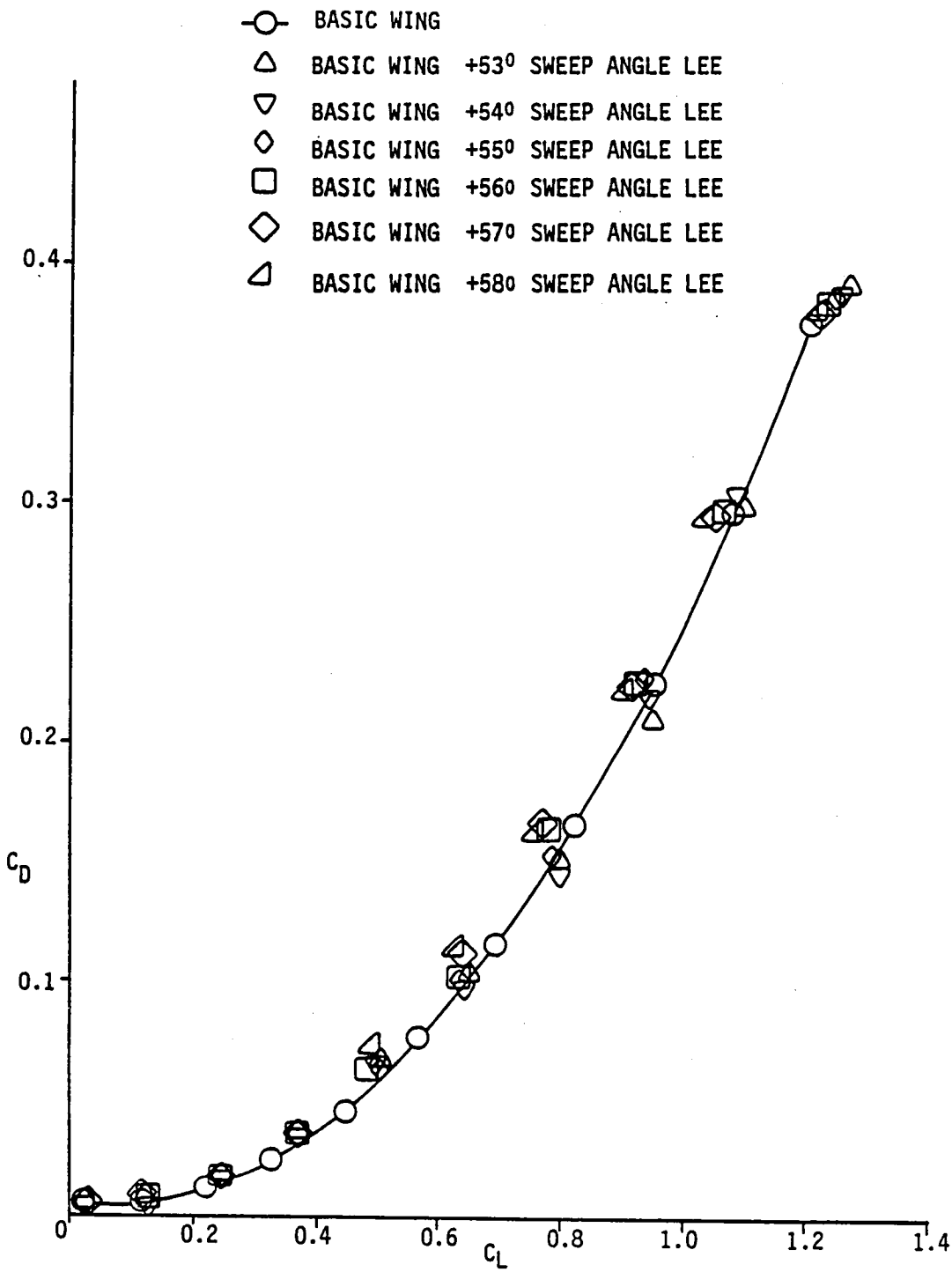

Fig. 3.5 Effect of LEE sweep angle on drag polar, η_{LEE} = 89%.

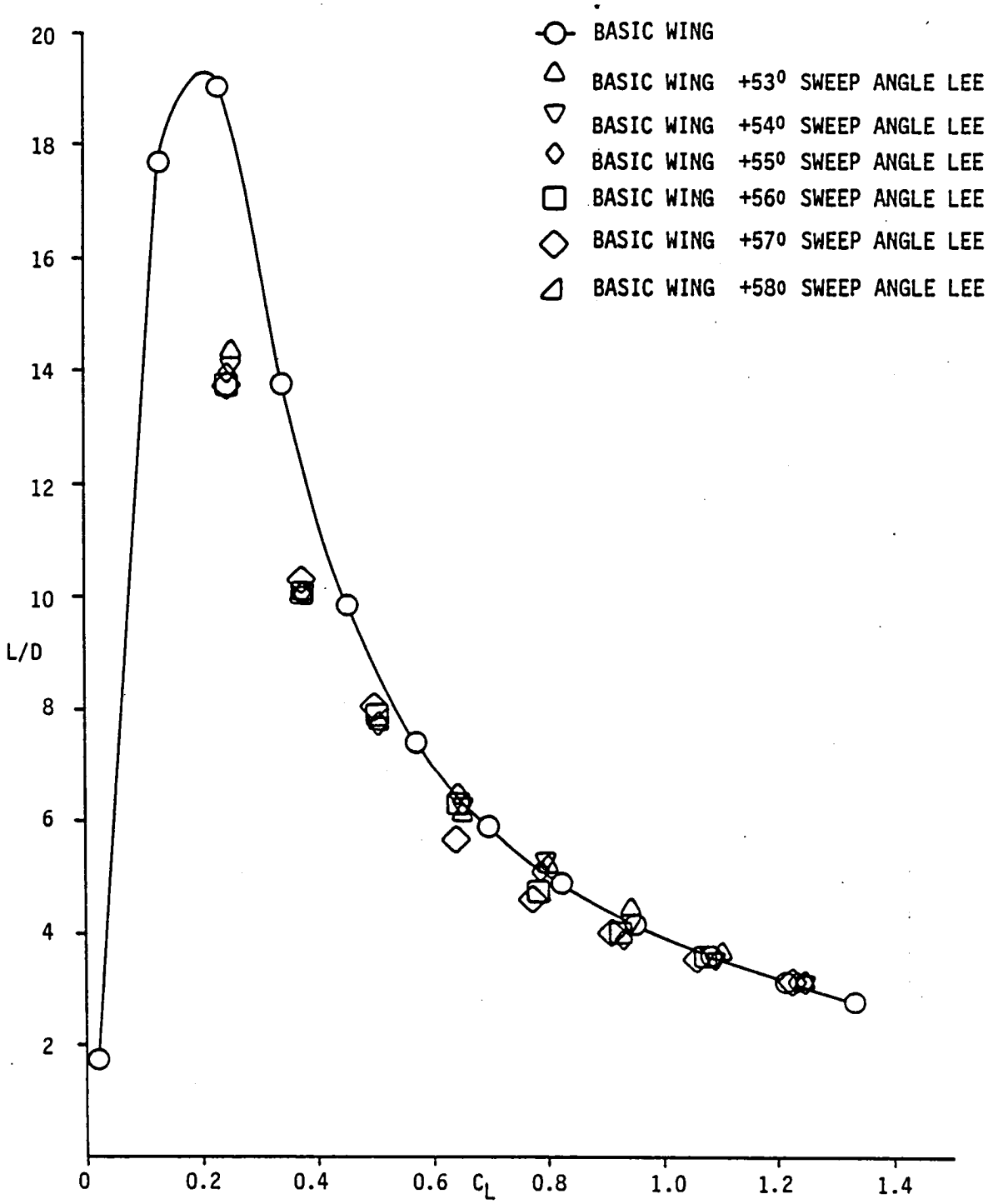

Fig. 3.6 Effect of LEE sweep angle on lift-to-drag ratio, η_{LEE} = 89%.

of other geometrical parameters such as chord and sweep angle simultaneously. In order to demonstrate these effects, a multi-variable plot shown in Fig. 3.7 was generated. This figure incorporates two aerodynamic variables (i.e., L/D, α) and three geometrical parameters (i.e., sweep angle, constant chord, area) in a single plot. In general, the figure shows that the LEE planform area does not have a considerable effect on lift-to-drag ratio over the entire range of angle of attack. Further, with regard to the comparison of the aerodynamic effectiveness of LEEs with different constant chord and sweep angles, the following conclusions are drawn based on equal LEE planform area. 1) At moderate angles of attack (6° to 10°), it appears that constant chord LEEs produce a better lift-to-drag ratio. 2) At 12° angle of attack, LEEs with sweep angles 57° to 55° generate better L/D, however outside this range constant chord LEEs achieve either the same or better improvements. 3) At 14° to 16° angle of attack, only low sweep angle LEEs appear to be more effective. However at higher angles of attack (18° to 20°), the figure shows a very slight change in L/D ratio, regardless of the LEE planform shape or area.

Evidently, these results coupled with the present study's design requirements (i.e., LEE with minimum area and chord) suggest that, 0.8" constant chord LEE has the aerodynamic potential of being selected as a candidate for the final LEE planform design. Further, 1.2" constant chord LEE also appears to be promising. Although this LEE benefits from 1.5 times larger area compared to 0.8" constant chord LEE, it produces

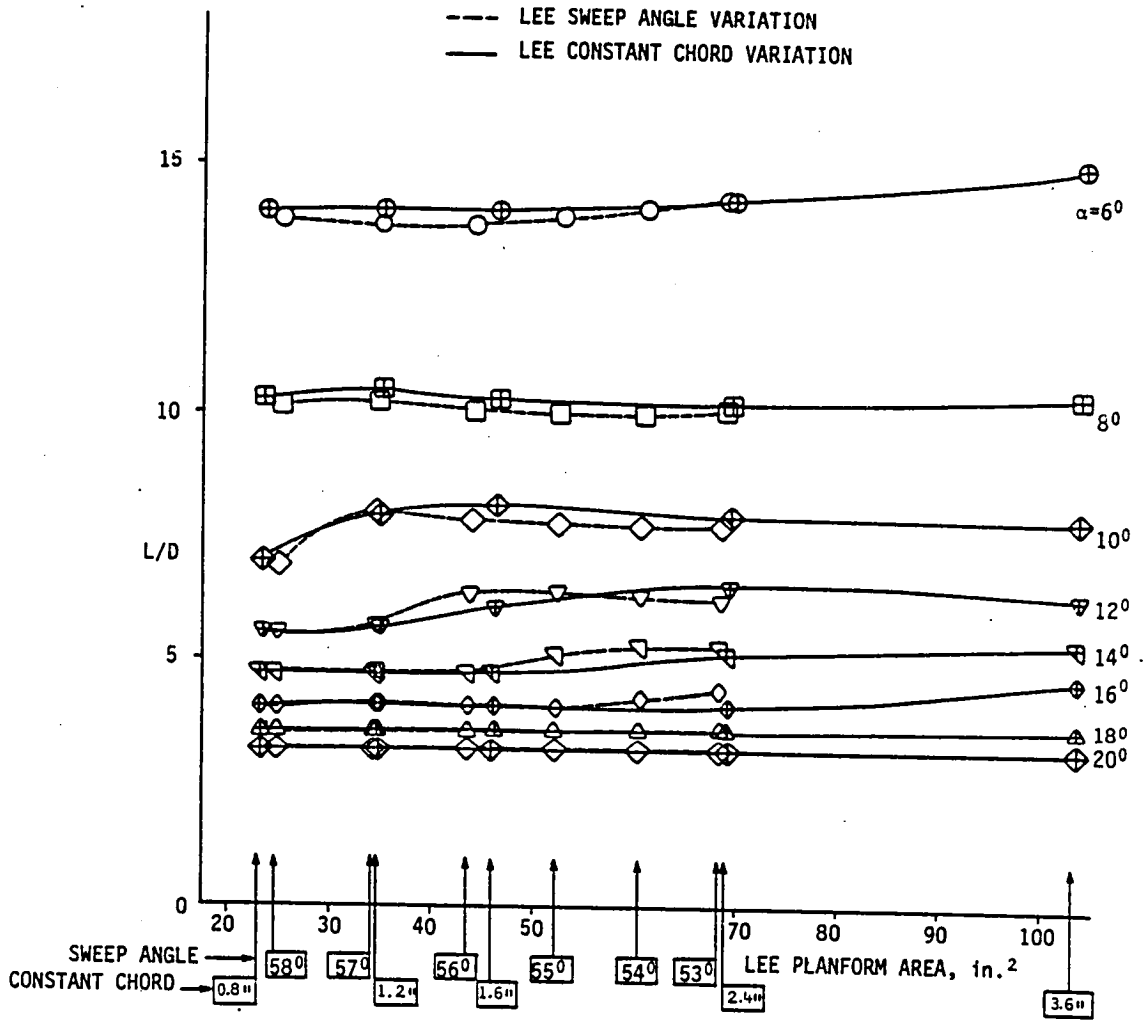

Fig. 3.7 Effect of LEE-planform geometrical-parameters on lift-to-drag ratio, η_{LEE} = 89%.

14.3% improvements in L/D at 10° and a slight increase at 8° and 12° angles of attack.

3.4 Span Extent

The selected LEE planforms which were used earlier in Secs. 3.2 and 3.3 to investigate the aerodynamic effect of constant chord and sweep angle, are employed here to study the same effects on reduced span extent. The selected LEE span extents included 12.11" and 8.07" which correspond to 75% and 50% of the wing-model semispan, respectively. Associated with each span extent, twelve LEE planforms (i.e., 4.8", 3.6", 2.4", 1.6", 1.2", and 0.8" constant chord, and 53°, 54°, 55°, 56°, 57°, and 58° sweep angle) are examined in this section. The VLM-SA estimates were generated by using the same number of horseshoe vortices on the wing model, however, 7-by-18 and 7-by-12 array of horseshoe vortices were used on LEE planforms with 75% and 50% span extent, respectively.

The VLM-SA analytical estimates of lift and drag coefficients for 75% and 50% span-extent LEEs with constant chord are plotted in drag polar form in Figs. 3.8 and 3.9, respectively. These two figures coupled with Fig. 3.2 (i.e., 89% span-extent LEE) show that in general beyond $C_{L,d}$, the reduction in the extent of the LEE's span causes an increase in drag at constant lift coefficients. It is interesting to note that the drag increase associated with a longer chord LEE is relatively substantial. Similar drag polar plots are shown in Figs. 3.10 and 3.11,

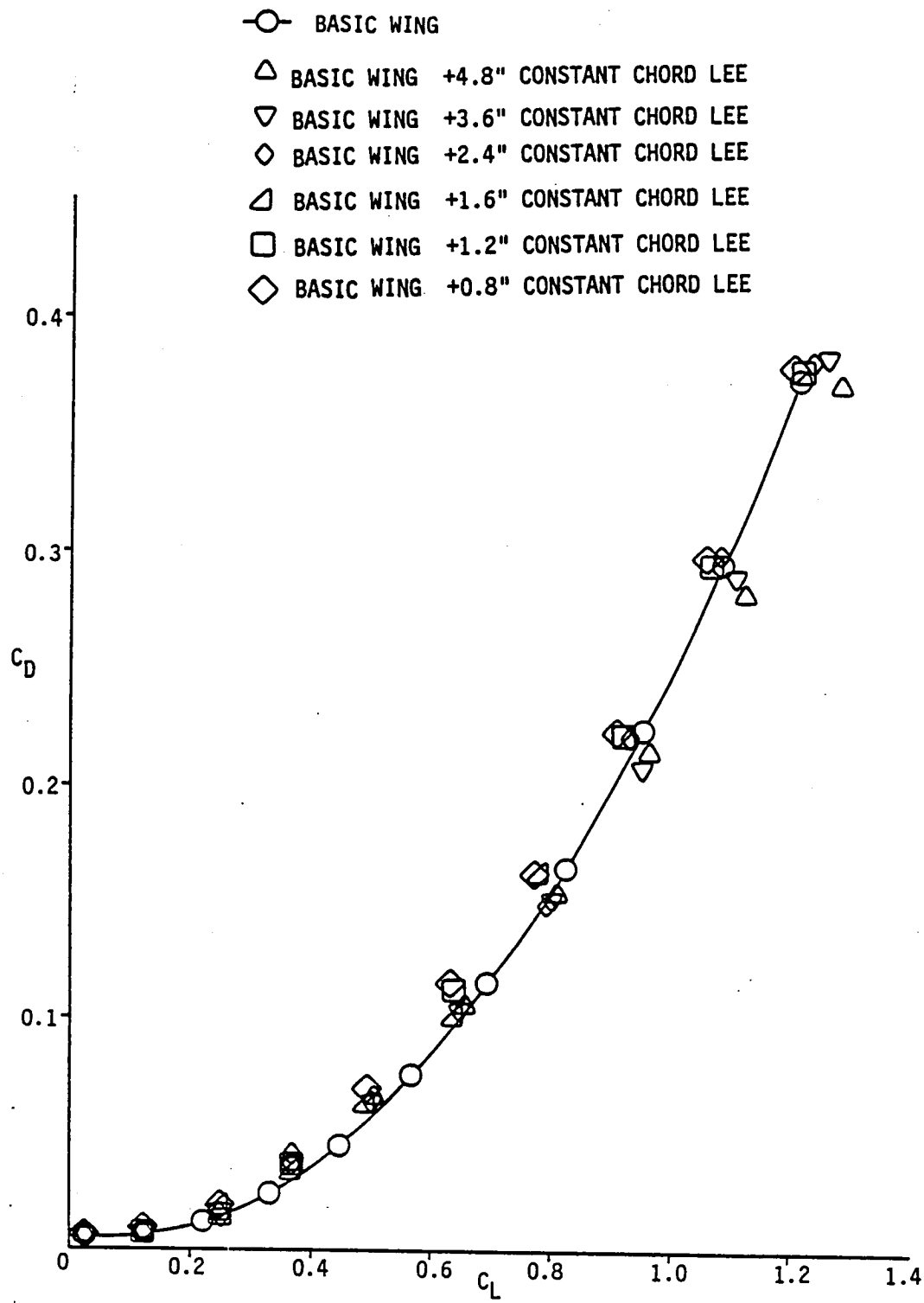

Fig. 3.8 Effect of constant chord length for LEE on drag polar, η_{LEE}= 75%.

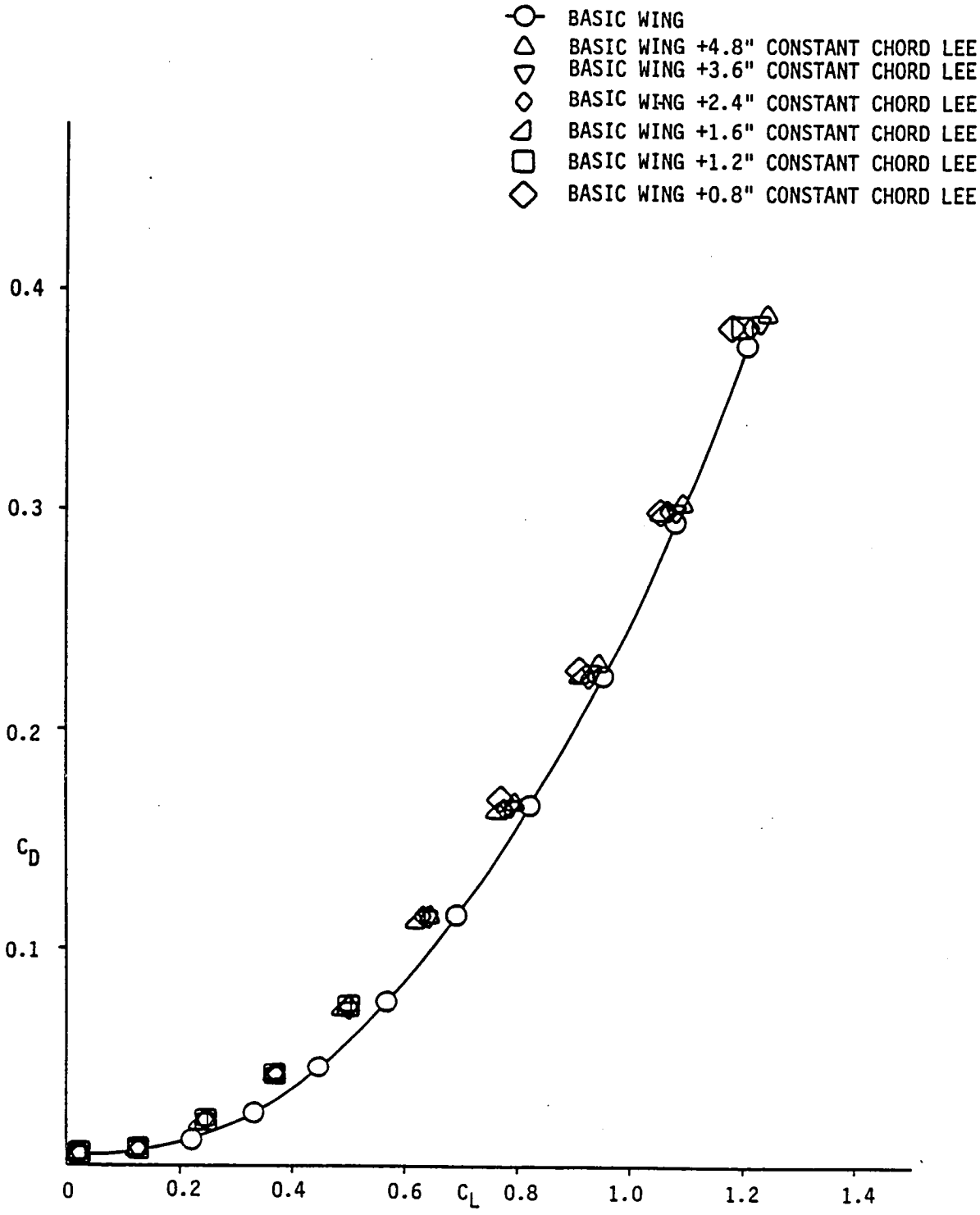

Fig. 3.9 Effect of constant chord length for LEE on drag polar, η_{LEE}=50%.

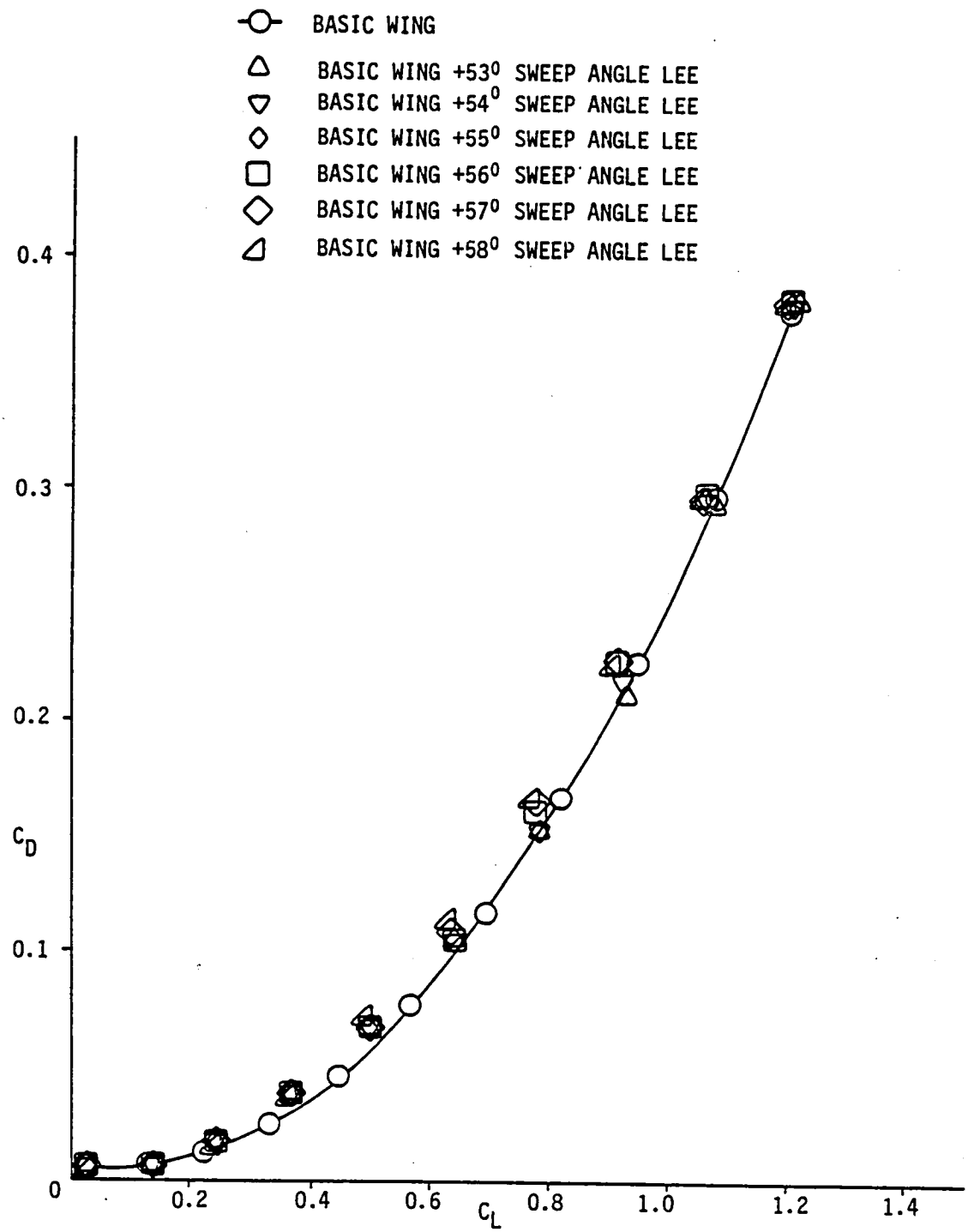

Fig. 3.10 Effect of LEE sweep angle on drag polar, η_{LEE}=75%.

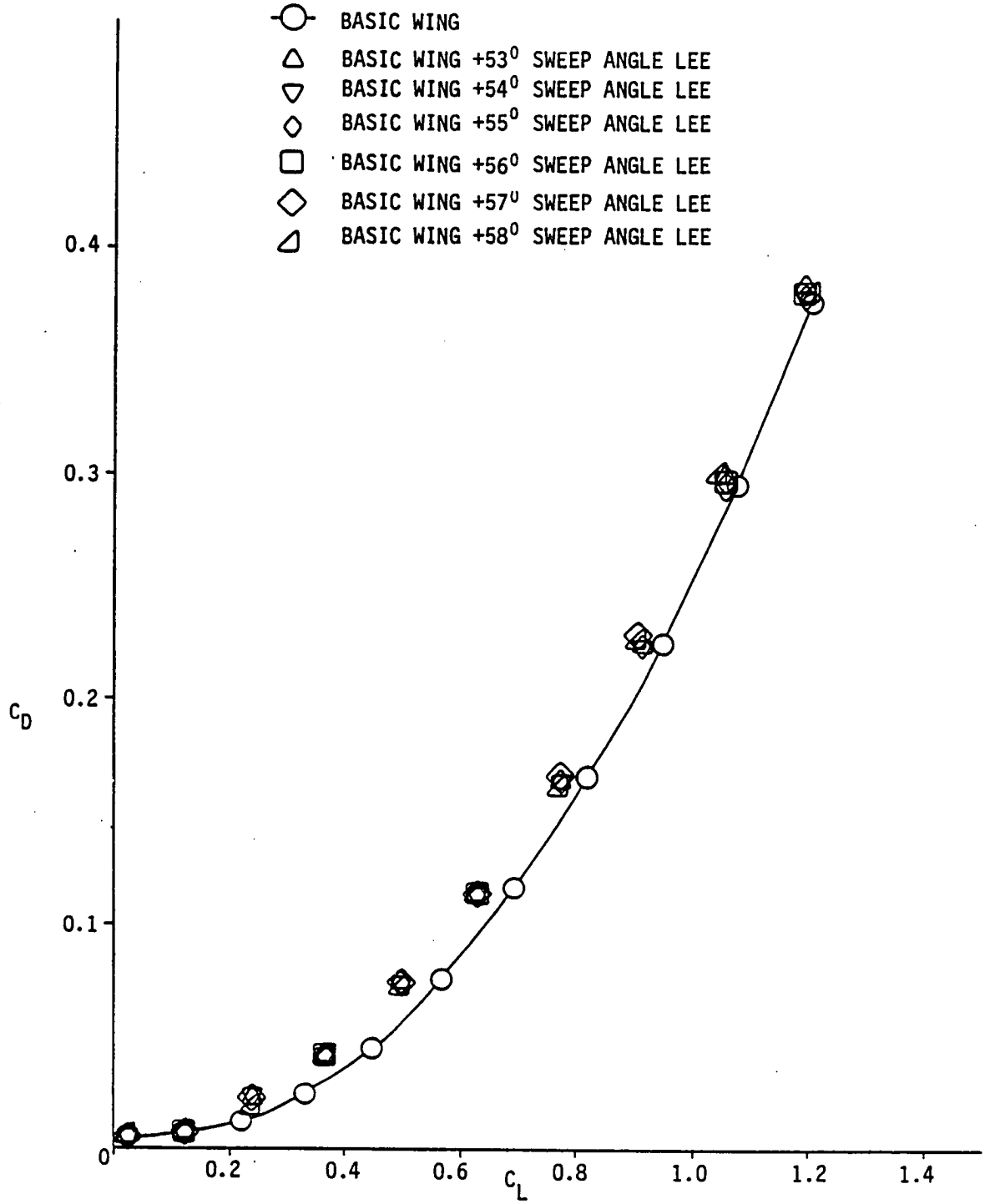

Fig. 3.11 Effect of LEE sweep angle on drag polar, η_{LEE}=50%.

respectively, for 75% and 50% span-extent LEEs with different sweep angles. These figures coupled with Fig. 3.5 (i.e., 89% span-extent LEE) also show a similar drag increase behavior at constant lift coefficients as the span-extent of the LEEs are reduced. Further, these figures show that the drag increase associated with LEEs having lower sweep angle is relatively higher. The following paragraph examines the aerodynamic effectiveness of different LEE planforms as a function of geometrical parameters by including the effects of LEE span extent, sweep angle, and constant chord.

Lift-to-drag ratio for 75% and 50% span LEE with different constant chord and sweep angle are plotted in Figs. 3.12 and 3.13, respectively. In general, a comparison of these figures with Fig. 3.7 shows that, a reduction in the LEE span extent decreases the L/D ratio in the α range of 6° to 12°, regardless of the LEEs planform shape and area. However, this effect appears to be insignificant as α increases beyond 14°. In regard to the comparison of the aerodynamic effectiveness of LEEs with different constant chord and sweep angle having the same planform area at a reduced span extent, the following conclusions are drawn. 1) 75% span LEEs (Fig. 3.12) conform with the conclusions drawn from 89% span LEE (see sec. 3.3, Fig. 3.7), and therefore they are not repeated here. 2) At 6° to 10° angle of attack, Fig. 3.13 shows that 50% span extent LEEs with constant chord appear to be aerodynamically slightly more effective. However, in general, the L/D variation as a function of LEE planform shape or area appears to be negligible throughout the examined

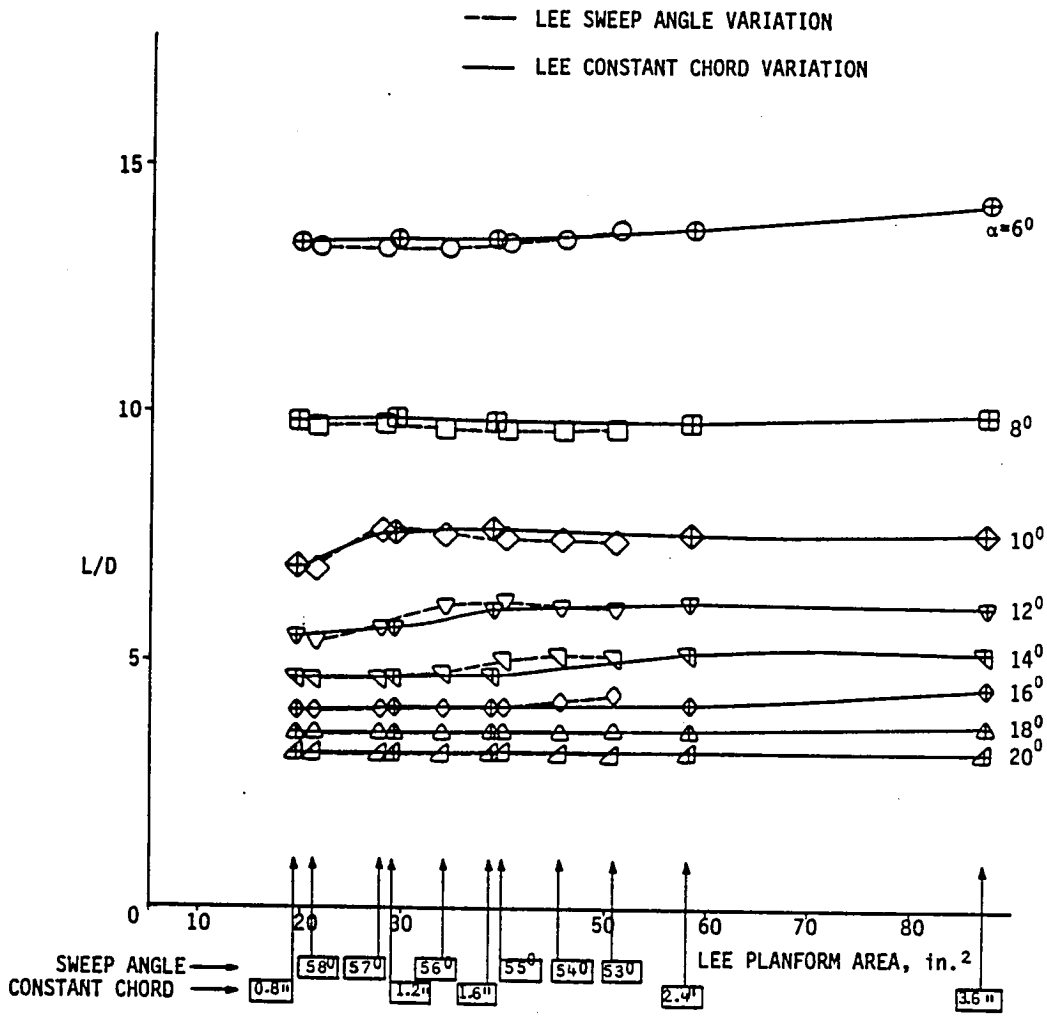

Fig. 3.12 Effect of LEE-planform geometrical-parameters on lift-to-drag ratio, η_{LEE}=75%.

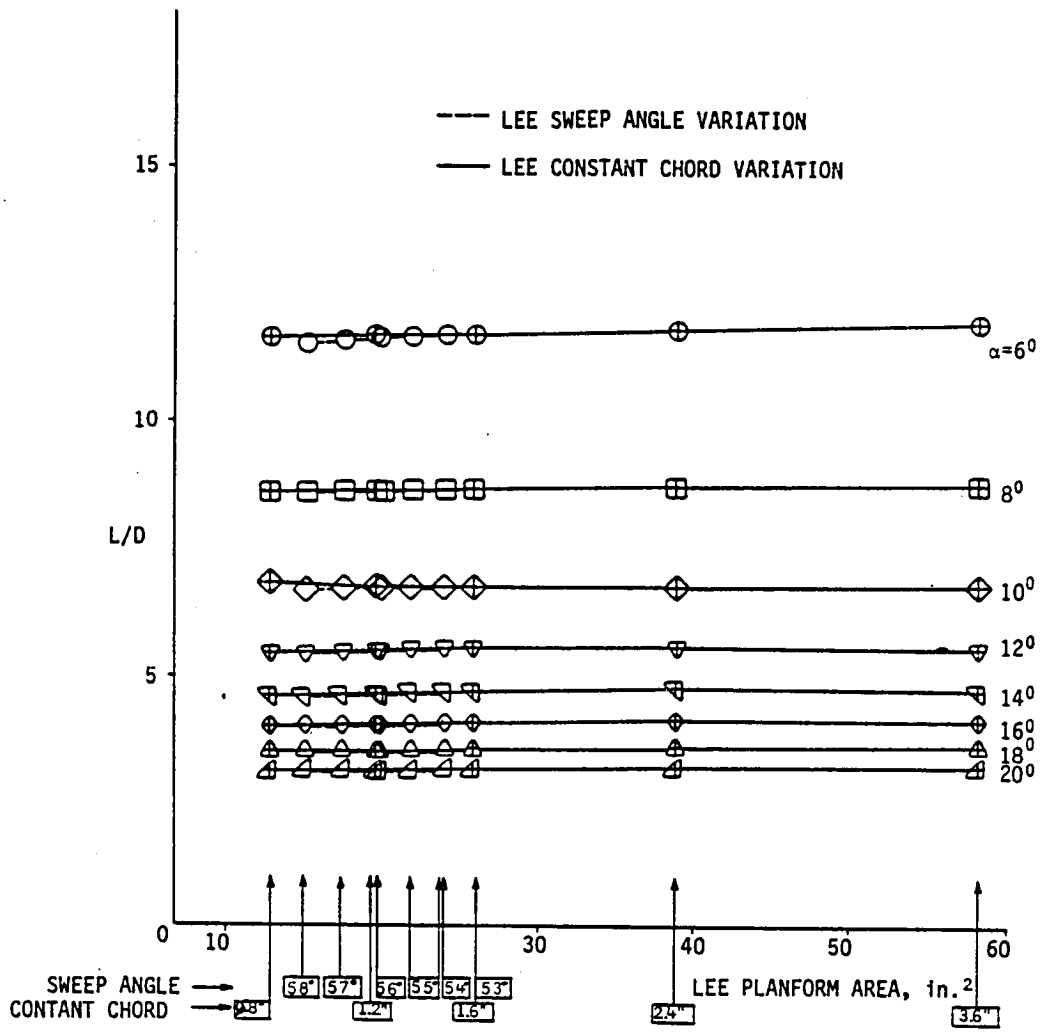

Fig. 3.13 Effect of LEE-planform geometrical-parameters on lift-to-drag ratio, η_{LEE}=50%.

α range. This is an interesting result. As shown in Fig. 3.13, although 3.6" constant chord LEE has 4.5 times larger planform area than the 0.8" constant chord, they both produce almost the same L/D ratio throughout the angle of attack range. Further, Fig. 3.14 shows the reduction in L/D ratio as the LEE span extent is decreased, for two different angles of attack, on the extreme LEE planform shapes. These results suggest that a minimum LEE chord at the inboard of the wing leading edges (i.e., apex region) is sufficient to yield an aerodynamically efficient LEE planform shape.

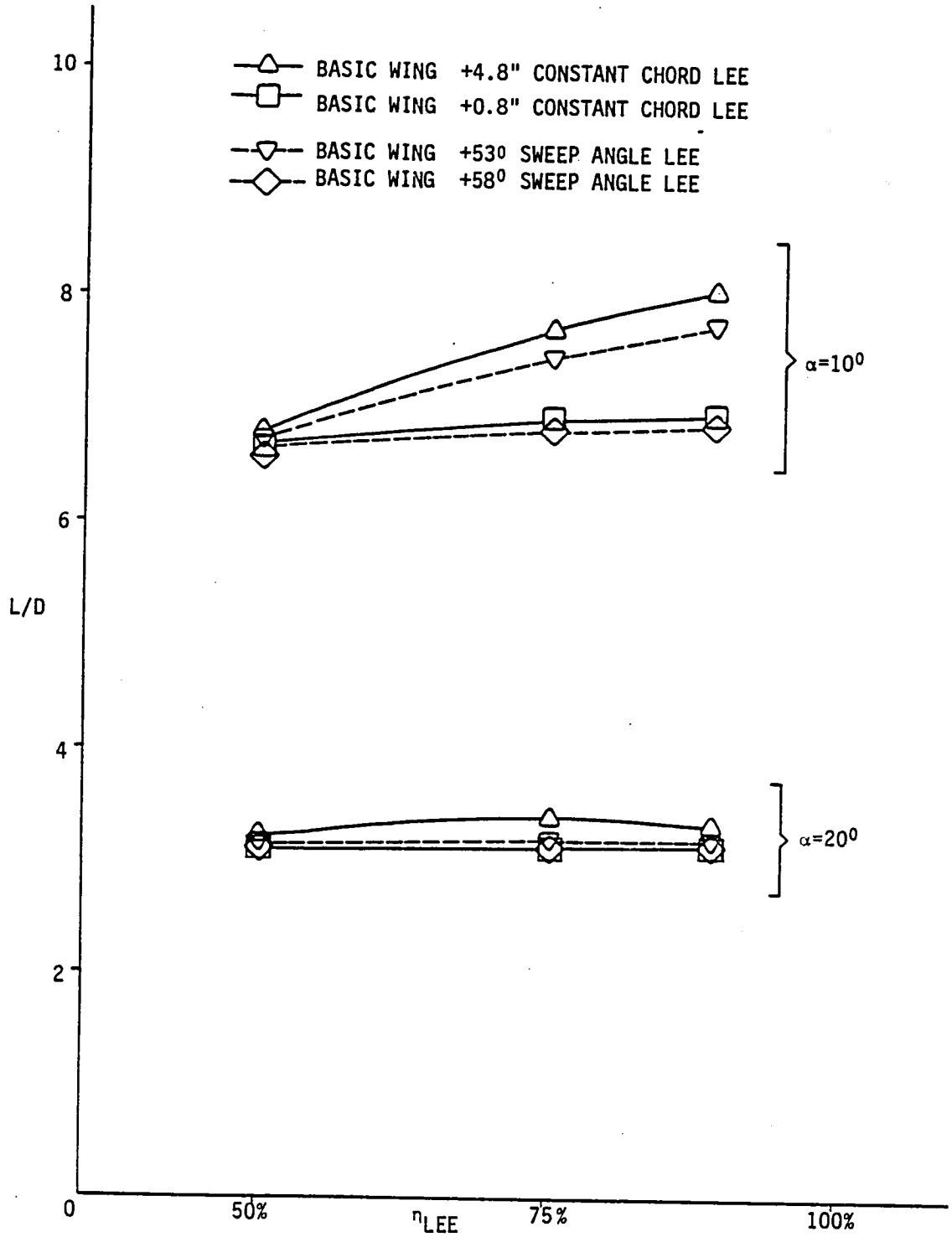

Fig. 3.14 Effect of LEE span extent on lift-to-drag ratio.

Chapter 4

RECOMMENDATIONS AND CONCLUSIONS

The present study demonstrated the applicability of a newly developed analytical design procedure for the determination of an aerodynamically efficient Leading-Edge Extension (LEE) for thick delta wings. Although, the procedure is general enough to incorporate the effects of pitching moment, this study considered only the aerodynamic performance of a cambered and twisted wing at high-subsonic speed. Through an examination of the available analytical tools, the PAN AIR and VLM-SA computer codes were employed to carry out the first application of the developed design procedure for the given wing of the present study. The following sections summarize the effectiveness of the analytical codes employed in this study as well as the resulting LEE effects.

4.1 Analytical Tools Effectiveness

1. The Pseudo-Stagnation Stream Surface (PSSS) solution associated with the wing model at the attached flow design condition was determined by employing the PAN AIR code.

2. The PAN AIR code was further employed to reexamine the accuracy of the determined PSSS solution. This investigation showed that resolving the problem with the PSSS in place resulted in a negligible influence on the aerodynamic pressures of the wing model at the attached flow design condition. Hence, it was concluded that the determined PSSS

solution is a good approximation of the dividing streamline surface.

3. An evaluation of the analytical capability of VLM-SA demonstrated that, at low-to-moderate lift coefficient, the code estimates of drag were in good agreement with experimental data for a thick delta wing. However, when a LEE was added as shown in Appendix B, the VLM-SA code over-estimated the drag in the lift coefficient range of about 0.05 to 0.80, because of the omission of suction pressures on the wing thickness. As a result, by analogy, it was concluded that the code estimates for drag would be too high in the present study of the wing-LEE configuration. Hence, throughout this study the aerodynamic effectiveness of different wing-LEE combinations were emphasized relative to one another rather than to the basic wing model.

4.2 LEE Aerodynamic Effectiveness

1. The analytical estimates obtained from VLM-SA code indicated that increasing the LEEs' constant chord reduces the total drag at moderate-to-high lift coefficient. However, no considerable improvement in L/D ratio was experienced with increasing constant chord size (i.e., increasing LEE planform-area) for the majority of the examined angles of attack.

2. At low and high lift coefficient, the variation of the LEEs' sweep angle had only a slight effect on the drag and lift characteristics of the wing-LEE combination. However, at moderate lift coefficients (i.e., 0.6 to 1.0), it was found that LEEs with lower sweep angle were more effective in reducing the drag. In general, based on

equal planform area, it was evident that constant chord LEEs produce either the same or better L/D ratio than LEES with different sweep angles for most of the examined angles of incidence.

3. Outboard reduction in the LEE span extent decreased the L/D ratio in the α range of 6.0° to 12°, regardless of the LEEs planform shape and area. However, this effect appeared to be insignificant beyond 14° angle of attack.

4. The design requirements of the present study, coupled with the results obtained for thirty-six different LEE planforms, suggest that the 0.8" constant-chord with 89% span extent has the aerodynamic potential of being selected as the best candidate for the final LEE planform design. Further, relative to the above LEE planform, the 1.2" constant-chord, with the same span extent, also appeared to be promising in achieving a better L/D ratio, especially at 10° angle of attack.

4.3 Concluding Remarks

It is firmly believed that the LEE concept has extensive drag-reduction capability that justifies further investigation. The principal research effort should be toward the selection of appropriate analytical tool(s) for the accurate determination of the PSSS at a given design flow-condition, as well as, the LEE planform optimization. Although efforts have been made to validate the results obtained in the present study wherever possible, it is recommended that the aerodynamic effectiveness of the resulting LEE be verified experimentally in a wind tunnel investigation.

ACKNOWLEDGMENTS

The first author expresses the highest appreciation to his advisors, Dr. Sushil K. Chaturvedi, of Old Dominion University, and Dr. John E. Lamar, of NASA/Langley Research Center, for substantial advice and assistance during the course of this investigation.

In particular, the author wishes to acknowledge his sincere gratitude to Dr. John E. Lamar of the National Transonic Facility Aerodynamics Branch (NTFAB), whose technical guidance, enthusiasm, skill, and continual moral support was vital to the success of this research effort. The author's appreciation is also extended to NTFAB fellow researchers, especially to Dr. Richard W. Barnwell, for providing him with the most pleasurable research environment as one could possibly ask.

REFERENCES

1. Wentz, W.H., Jr., "Effects of Leading-Edge Camber on Low-Speed Characteristics of Slender Delta Wings," NASA CR-2002, October 1972.

2. Rao, D.M., "Exploratory Subsonic Investigation of Vortex Flap Concept on Arrow Wing Configuration," NASA CP 2108 (Part I), November 1979.

3. Henderson, W.P., "Effects of Wing Leading-Edge Radius and Reynolds Number on Longitudinal Aerodynamic Characteristics of Highly Swept Wing-Body Combinations at Supersonic Speeds," NASA TN D-8361, December 1976.

4. Bobbitt, P.J. "Modern Fluid Dynamics of Subsonic and Transonic Flight," AIAA Paper 80-0861, May 1980.

5. Rao, D.M., "Leading-Edge "Vortex Flaps" for Enhanced Subsonic Aerodynamics of Slender Wings," ICASE-80-13.5, October 1980.

6. Johnson, T.D., Jr. and Rao, D.M., "Experimental Study of Delta Wing Leading-Edge Devices for Drag Reduction at High Lift," NASA CR-165846, February 1982.

7. Tingas, S.A. and Rao, D.M., "Subsonic Balance and Pressure Investigation of a 60 deg. Delta Wing with Leading-Edge Devices," NASA CR-165923, May 1982.

8. Yip, L.P. and Murri, D.G., "Effects of Vortex Flaps on the Low-Speed Aerodynamic Characteristics of an Arrow Wing," NASA TP-1914, November 1981.

9. Rao, D.M., "Leading-Edge Vortex Flaps Experiments on a 74 deg. Delta Wing," ODU Research Foundation, NASA CR-159161, November 1979.

10. Wilson, H.A. Jr. and Lovell, J.C., "Full-Scale Investigation of the Maximum Lift and Flow Characteristics of an Airplane Having Approximately Triangular Planforms," NASA RM No. L6K20, February 1947.

11. Lamar, J.E. and Campbell, J.F., "Recent Studies at NASA-Langley of Vortical Flows Interacting with Neighboring Surfaces," AGARD Symposium on Aerodynamics of Vortical Type Flows in Three-Dimensions, Paper No. 10, April 1983.

12. Rao, D.M., "Vortical Flow Management for Improved Configuration Aerodynamics - Recent Experiences," AGARD Symposium on Aerodynamics of Vortical Type Flows in Three-Dimensions, Paper No. 30, April 1983.

13. Johnson, F.T., Lu, P., Tinoco, E.N., and Epton, M.A., "An Improved Panel Method for the Solution of Three-Dimensional Leading Edge Vortex Flows," NASA CR-159173, June 1979.

14. Sidwell, K.W., Baruah, P.K., and Bussoletti, J. E., "PAN-AIR A Computer Program for Predicting Subsonic or Supersonic Linear Potential Flows about Arbitrary Configurations Using a Higher Order Panel Method," NASA CR-3252, May 1980.

15. Lamar, J.E., and Gloss, B.B., "Subsonic Aerodynamic Characteristics of Interacting Lifting Surfaces with Separated Flow Around Sharp Edges Predicted by a Vortex-Lattice Method," NASA TN D-7921, September 1975.

16. Hall, J.F., and Neuhart, D.H., and Walkley, K.B., "An Interactive Program for Manipulation and Display of Panel Method Geometry," NASA CR-166098, March 1983.

17. Polhamus, E.C., "Prediction of Vortex-Lift Characteristics by a Leading-Edge Suction Analogy," Journal of Aircraft, Vol. 18, No. 4, April 1971, pp. 193-199.

18. Lamar, J.E. and Herbert, H.E., "Production Version of the Extended NASA-Langley Vortex Lattice FORTRAN Computer Program," Vol. I Source Code. NASA TM-83303, April 1982.

19. Herbert, H.E. and Lamar, J.E., "Production Version of the Extended NASA-Langley Vortex Lattice FORTRAN Computer Program," Vol. II Source Code. NASA TM-83304, April 1982.

20. Rowe, W.S., Winther, B.A., and Redman, M.C., "Prediction of Unsteady Aerodynamic Loadings Caused by Trailing Edge Surface Motions in Subsonic Compressible Motions in Subsonic Compressible Flow Analysis and Results," NASA CR-2003, June 1972.

APPENDIX A. PAN AIR CODE

The intended purpose of this Appendix is to discuss briefly some of the capabilities and the limitations of the PAN AIR code. Also, the degree of accuracy of the determined PSSS solution is examined.

A.1 Discussion

PAN AIR code is a boundary-value problem solver for the Prandtl-Glauert equation

$$(1-M^2_\infty)\,\phi_{xx} + \phi_{yy} + \phi_{zz} = 0$$

Thus, PAN AIR's numerical solutions embody all the limitations inherent in this approximate representation of the flow field. Such limitations include steady, inviscid, irrotational, subsonic and supersonic flows. This higher order panel code uses linear source and quadratic doublet strength distribution to determine the flow field.

PAN AIR aerodynamic analysis capability consists of ability to: a) calculate pressure distribution and velocity components at any point on the surface of a configuration and b) calculate forces and moments both on the configuration as a whole and on specified portions of the configuration. This potential flow code is capable of employing survey networks which can be used to determine the velocity components at any point away from the configuration surface. In addition to the above, the PAN AIR code has the Influence Coefficient (IC)-update capability.

This capability, enables one to examine configurations which differ from the ones already processed in a limited fashion with respect to geometry. In this process a configuration surface is partitioned into several networks, with one or more tagged "updatable" in the original submission. The subsequent run, with any change (i.e., size, location) in the updatable networks, can utilize some of the unaffected calculations which have been performed and saved from the original execution.

A.2 PSSS Validation Test

As discussed in Chap. 2 of the present study, the PSSS solution was determined for the wing model at the attached flow design condition by the PAN AIR code. As part of the present study, it appeared necessary to examine the accuracy of the determined PSSS solution. This test was conducted by employing the PAN AIR code once again to model the wing-PSSS combination at the same attached flow design condition used in the present study to determine the PSSS solution. Although the modeled PSSS is specified as being a lifting surface, Fig. A.1 shows that its presence has little effect on the pressure distribution over several typical sections of the wing upper and lower surfaces. Also, as shown in Fig. A.2, the lifting pressure across the PSSS appears small at the same typical sections, especially away from the PSSS leading-edge. From these results, it is evident that the attachment of the PSSS solution, does not have a considerable influence on the performance of the wing model at the attached flow design condition. Therefore, it is concluded

that the determined PSSS solution is close to the actual dividing stream surface (i.e., pseudo-stagnation stream surface).

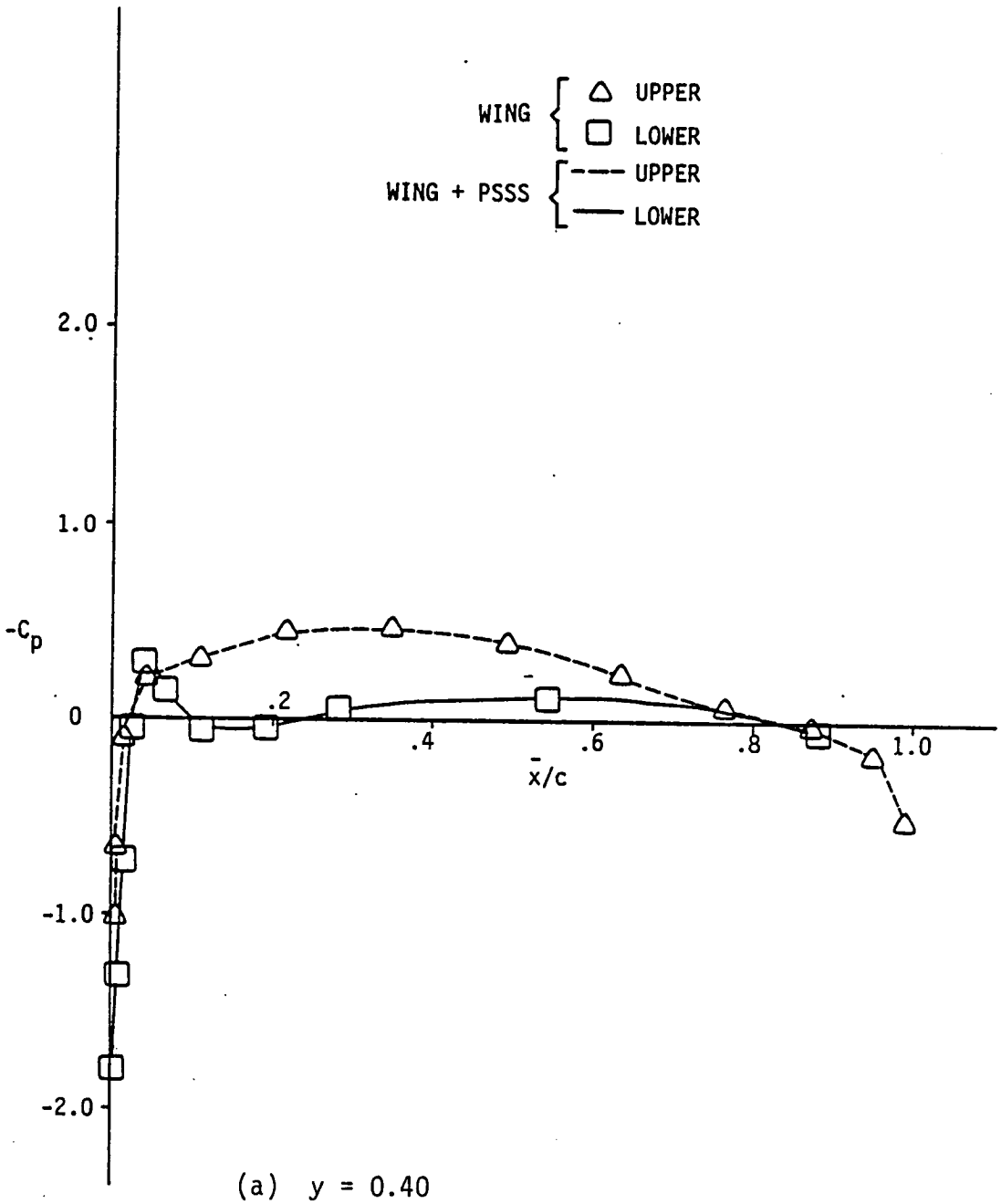

(a) $y = 0.40$

Fig. A.1 Chordwise pressure distribution of wing and wing-PSSS combination at $\alpha = 6.0^{o}$ and $M = 0.8$.

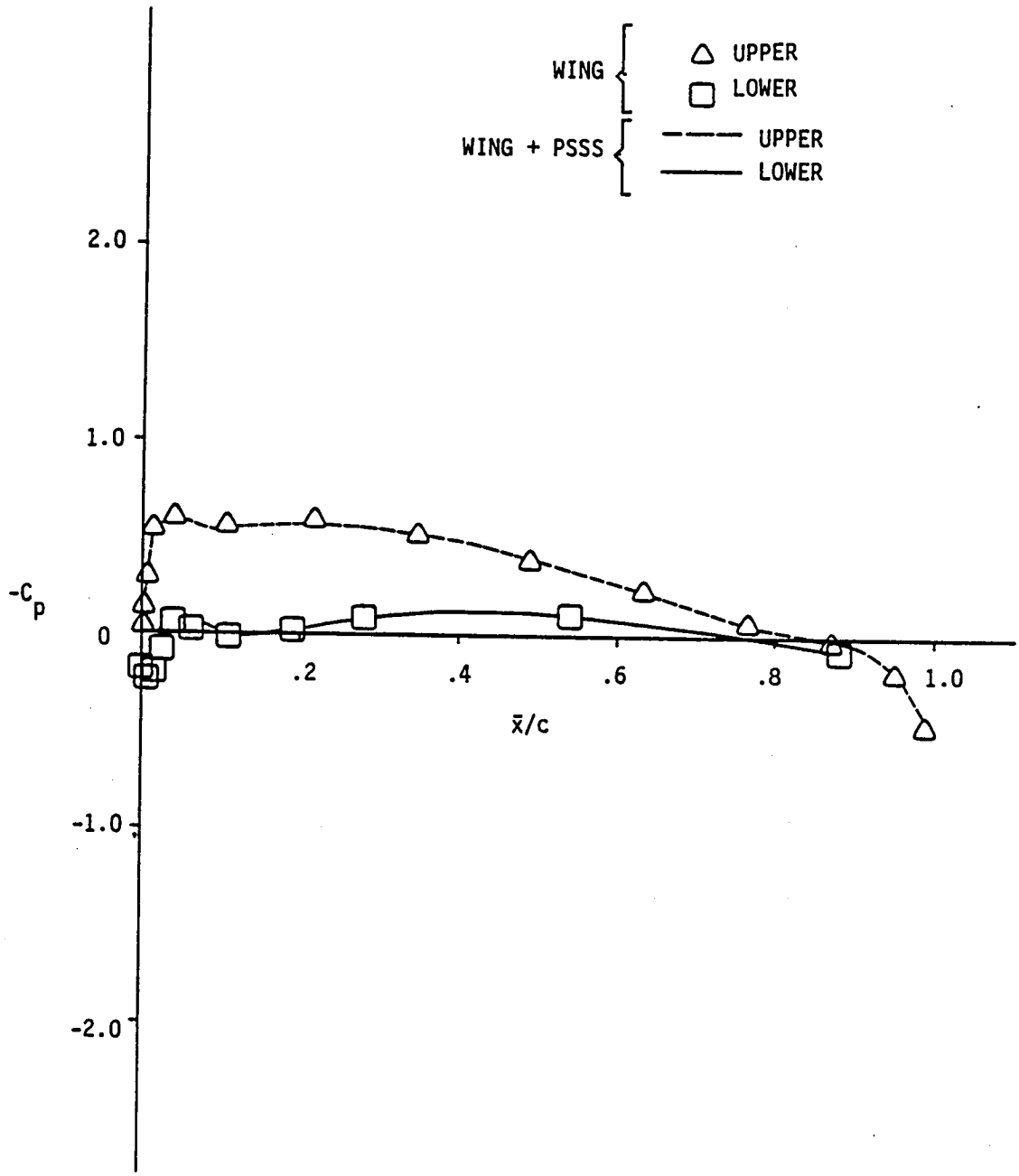

(b) y = 5.67

Fig. A.1 Continued.

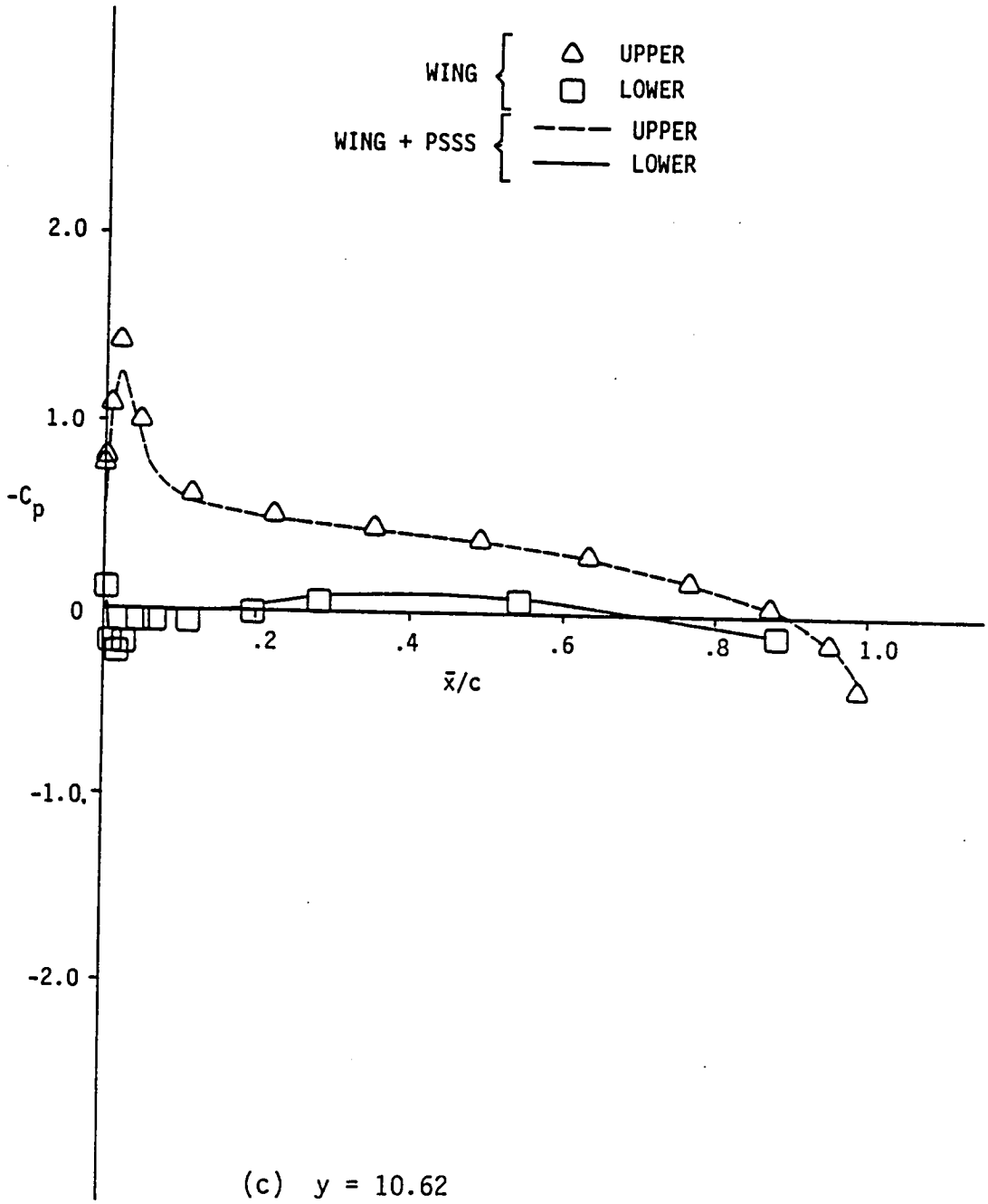

(c) y = 10.62

Fig. A.1 Continued.

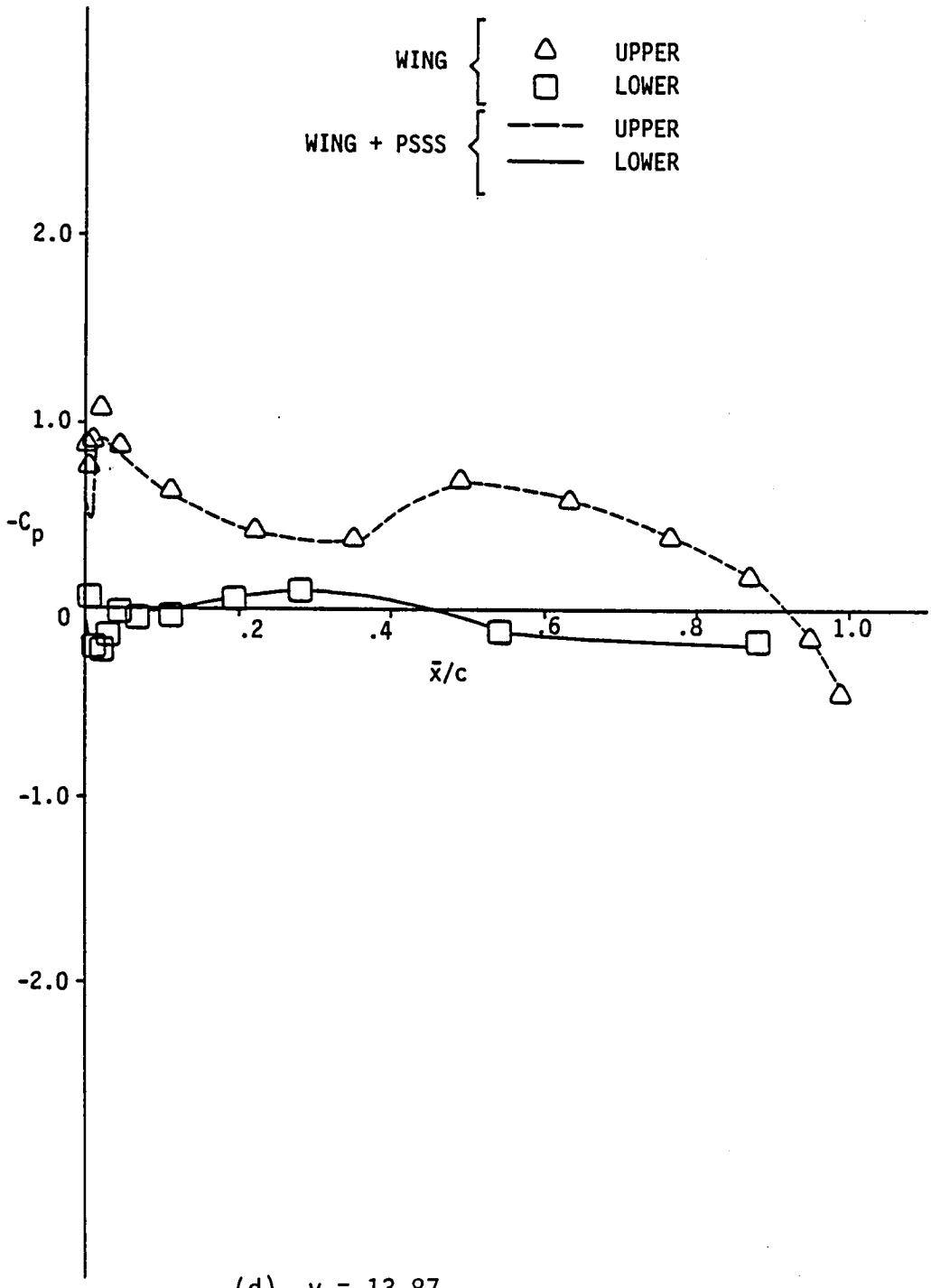

(d) y = 13.87

Fig. A.1 Concluded.

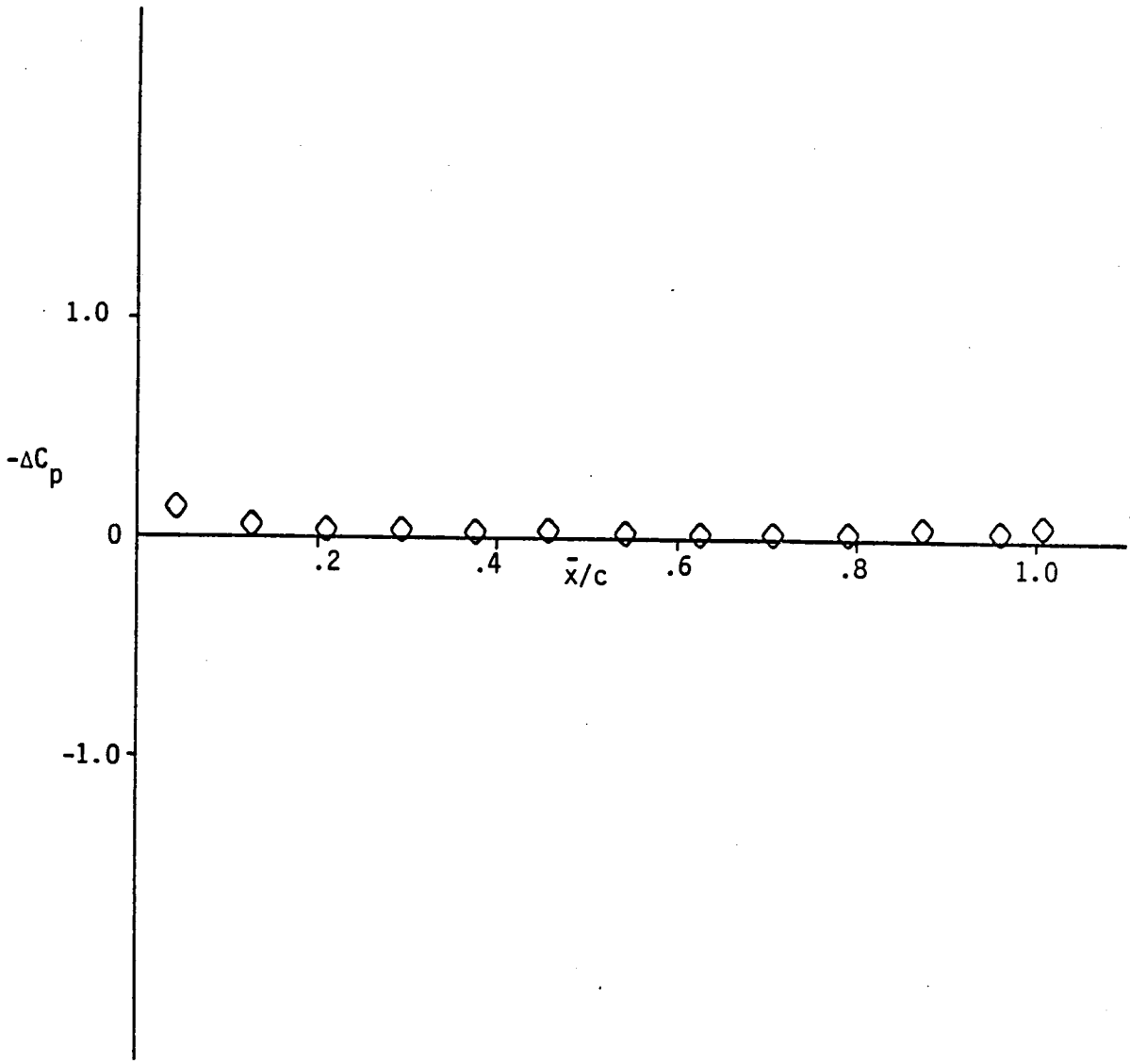

(a) y = 0.40

Fig. A.2 Net lifting pressure coefficient across the PSSS at $\alpha = 6.0^0$ and M = 0.8.

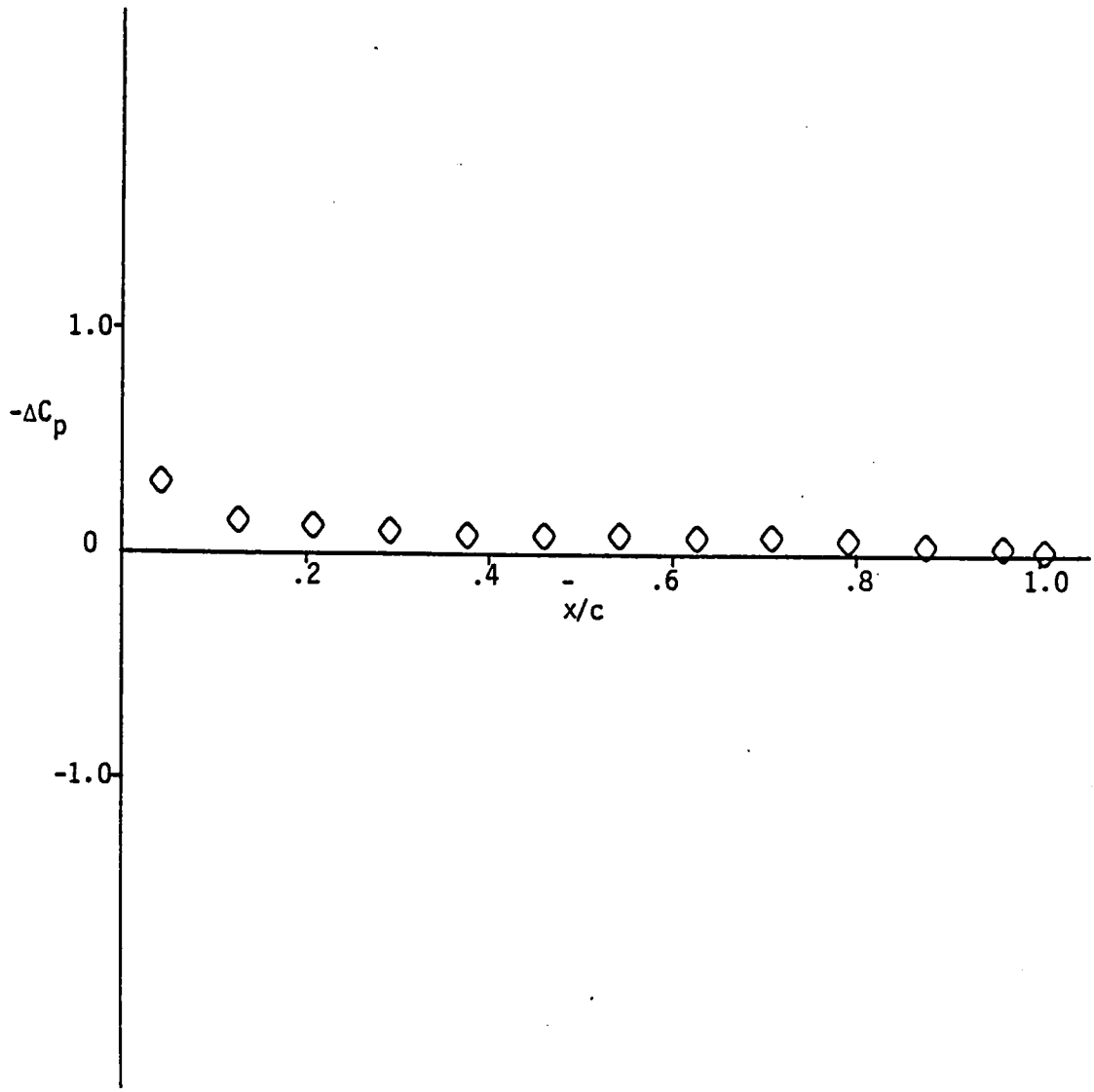

(b) y = 5.67

Fig. A.2 Continued.

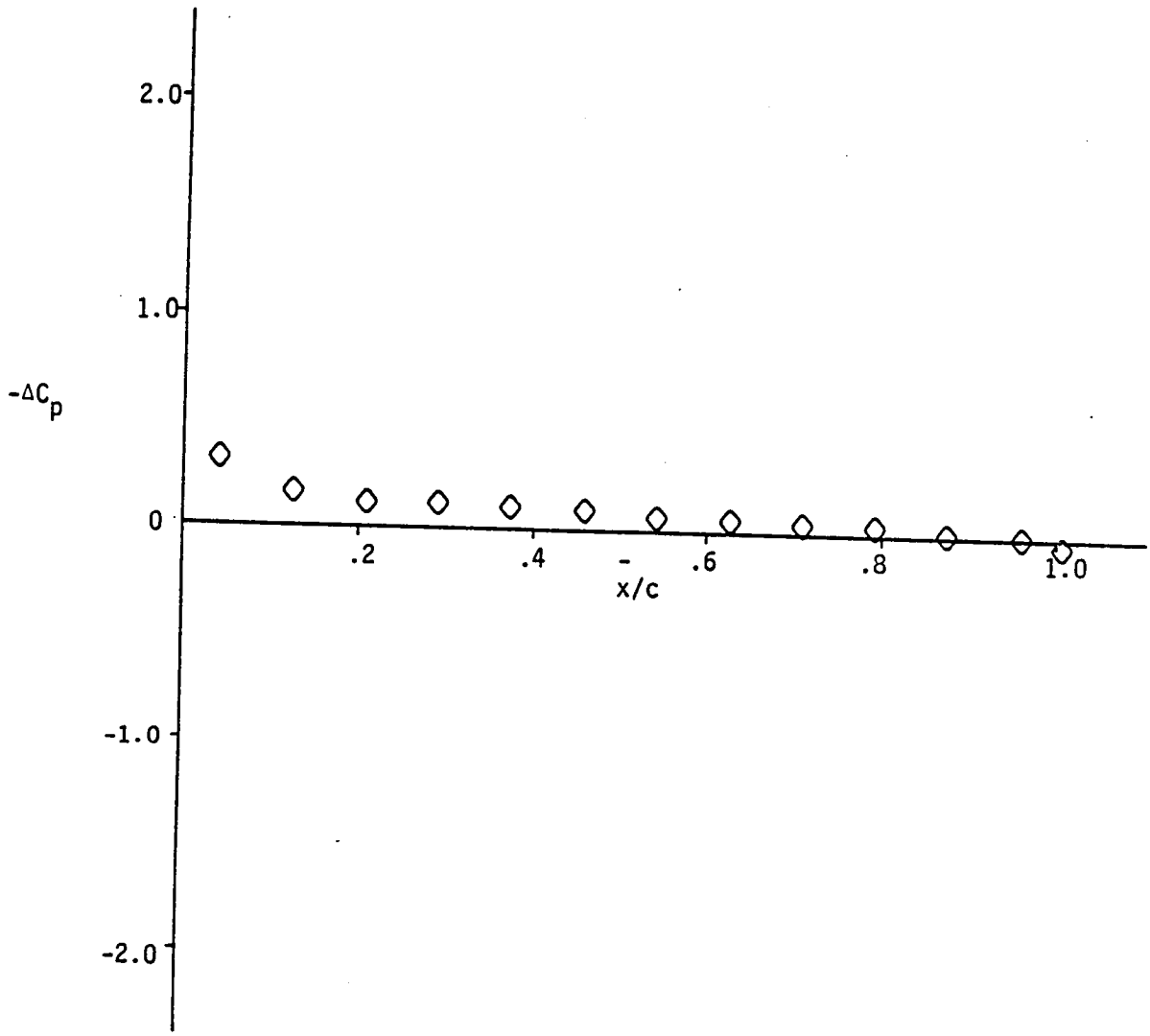

(c) y = 10.62

Fig. A.2 Continued.

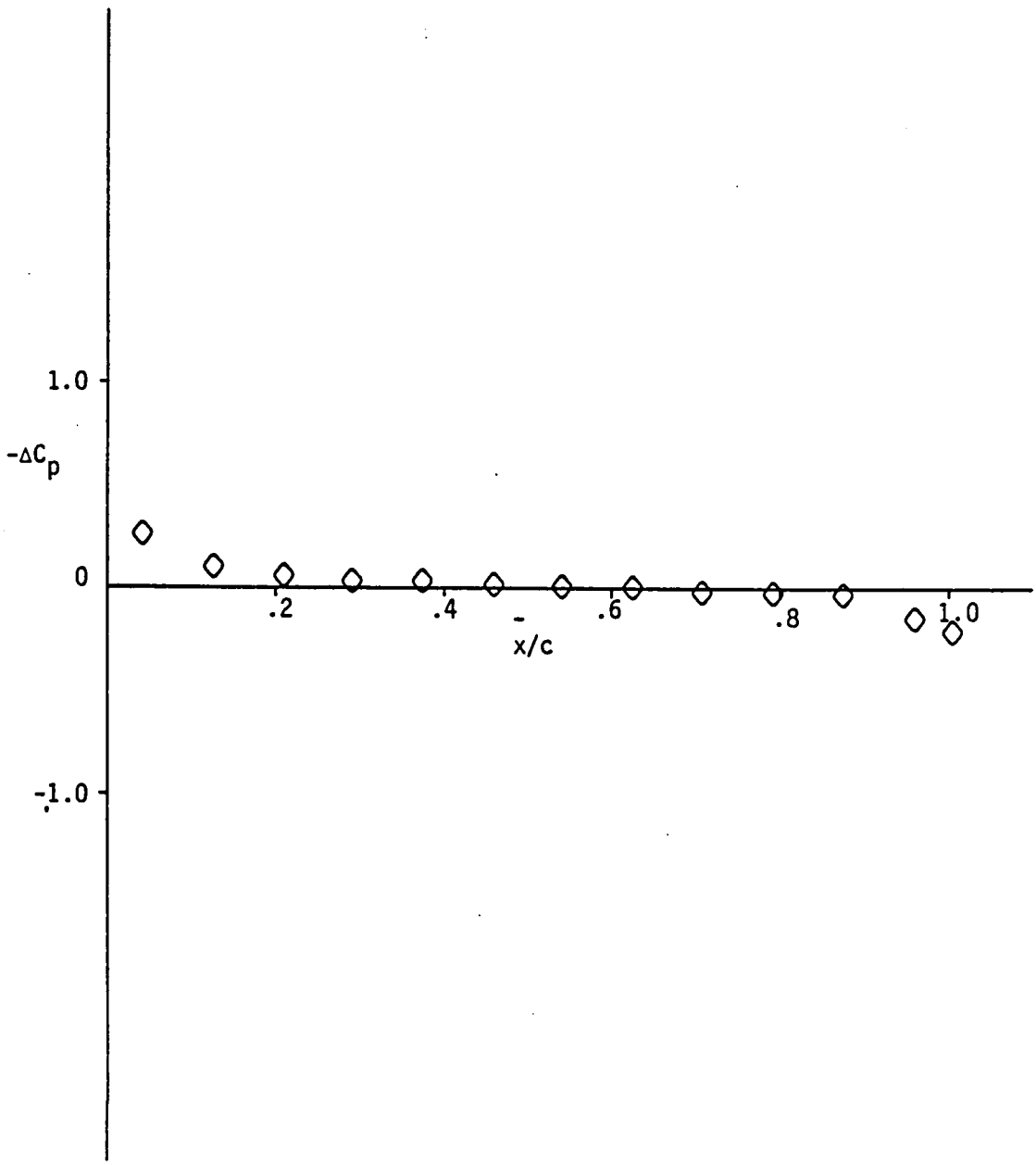

(d) y = 13.87

Fig. A.2 Concluded.

APPENDIX B. VLM-SA CODE

This Appendix includes a discussion on the VLM-SA methodology by highlighting some of the code capabilities and limitations in Sec. B.1. Also, the computer programs developed to generate the required local angles of attack for twisted and cambered wing and the LEE surface are listed in Sec. B.2. Lastly, results and a discussion on VLM-SA evaluation is presented in Sec. B.3.

B.1 Discussion

Theoretically, the conventional vortex lattice method is incapable of determining the aerodynamic characteristics of a wing configuration having leading-edge vortex flow. However, to overcome this limitation Lamar and Gloss [15] of NASA Langley have developed a computer code which couples the conventional method with suction analogy concept (VLM-SA). The suction analogy [17] states that the attached flow leading edge suction force which no longer acts in the chord plane when the leading-edge flow separates, is reoriented normal (rotated 90°) to the upper surface by the vortex flow action, thereby producing an additional force. This force is the aerodynamic force associated with the leading edge vortex flow. The VLM-SA code calculates this force and its contribution to lift, drag, and pitching moment. Then, these contributions are added to the potential flow results to find the total vortex induced forces and moments.

The VLM-SA code was extended to account for twist and camber (called VLM mark 4.0 version) as reported by Lamar/Herbert in refs. 18 and 19. VLM mark 4.9, the latest version of VLM-SA code, is capable of accounting for the effect of leading-edge radii as well. However, it does not provide pressure loading information. Although, the code neglects the effect of thickness, there have been techniques devised to include them [20].

The latest version of VLM-SA code is employed in the present study. The code aerodynamic analysis capability consists of ability to estimate overall potential flow, as well as, vortex flow induced forces and moments on complex planforms at subsonic speeds. Figure B.1, shows three types of flow situations considered by the code. These are: 1) full leading-edge suction (attached flow), 2) zero leading-edge suction (attached flow), and 3) zero leading-edge suction (vortex flow). All predicted results presented in this thesis correspond to the zero leading-edge suction with vortex flow.

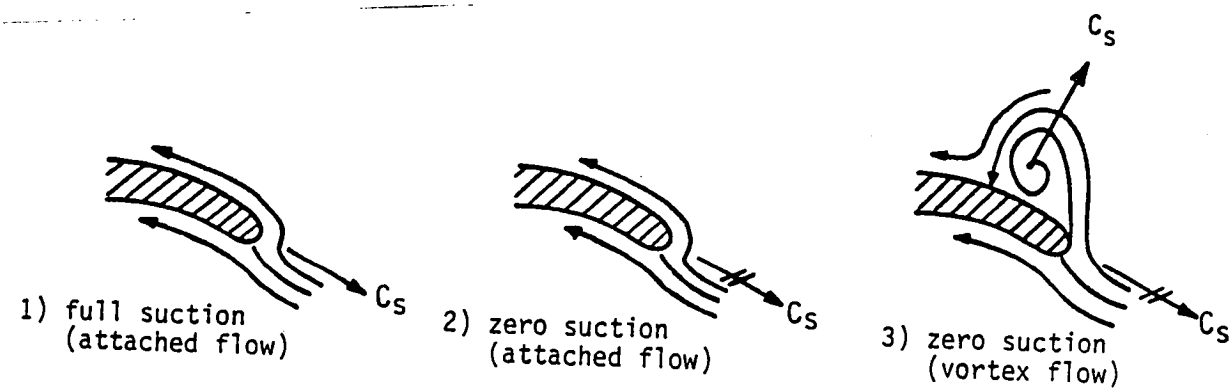

Fig. B.1 Theoretical flow mechanisms employed in the extended VLM-SA computations.

B.2 LOCAL ANGLES OF ATTACK CALCULATIONS

COMPUTER PROGRAMS LISTING

```
**********************************************************************
* IN ORDER TO EMPLOY THE VLM-SA CODE IN THE PRESENT STUDY, THIS COMPUTER  *
* PROGRAM HAD TO BE DEVELOPED.  THE PURPOSE OF THIS PROGRAM IS TO GENERATE *
* THE REQUIRED LOCAL ANGLES OF ATTACK (SLOPES) FOR THE GIVEN THICK WING   *
* GEOMETRY, WITH CAMBER AND TWIST, ALONG THE MEAN CAMBER SURFACE.         *
*       THIS PROGRAM IS SUMMERIZED INTO THE FOLLOWING FOUR STEPS.         *
* I) IT INTERPOLATES THE Z-COORDINATES OF THE WING TOP AND BOTTOM SURFACES *
* AT THE SAME X-COORDINATES STARTING FROM THE LEADING EDGE AND ENDING AT  *
* THE TRAILING EDGE OF EACH CHORDWISE STATION. THIS PROCESS IS REPEATED   *
* IN A SEQUENTIAL MANER STARTING FROM THE WING ROOT CHORD AND PROCEEDING  *
* TOWARD THE TIP STATION.                                                 *
* II) IT COMPUTES THE AVERAGE Z-COORDINATES AND THEREBY OBTAINING THE COOR-*
* DINATE POINTS OF THE MEAN CAMBER LINE ASSOCIATED WITH DIFFERENT CHORDWISE*
* STATIONS.                                                               *
* III) IT CALCULATES THE SLOPES ALONG THE MEAN CAMBER LINES TO SECOND     *
* DEGREE OF ACCURACY. THEN,                                               *
* IV) IT INTERPOLATES TO DETERMINE THE DESIRED NUMBER OF SLOPES AT THE CON-*
* TROL POINT OF EACH ELEMENTAL PANEL ON THE MEAN CAMBER SURFACE AS REQUIRED*
* BY VLM-SA CODE.                                                         *
*       -------FURTHER COMMENTS WILL BE GIVEN WITHIN THE-------           *
*              -------PROGRAM AS NEED RISES.-------                      *
**********************************************************************

C                    ==========LIST OF VARIABLES==========

C  XT, ZT   =X-COORDINATE, Z-COORDINAYE OF WING TOP SURFACE.
C  XB, ZB   =X-COORDINATE, Z-COORDINATE OF WING BOTTOM SURFACE.
C  Y        =Y-COORDINATE OF WING TOP AND BOTTOM SURFACES.
C  Z        =Z-COORDINATE OF THE WING BOTTOM SURFACE CORRESPONDING TO
C            THE SAME X-COORDINATE AS THE UPPER SURFACE.
C  NS       =NUMBER OF SPAN STATIONS.
C  NODE     =NUMBER OF CHORD STATIONS.
C  ZMCAM    =Z-COORDINATE OF THE MEAN CAMBER LINE ASSOCIATED WITH DIFFERENT
C            WING SECTION.
C  CHORD    =WING LOCAL CHORD.
C  CHORDND  =DESIRED NUMBER OF CHORD STATIONS.
C  LCHORD   =FRACTION OF WING LOCAL CHORD.
C  SPAN     =WING SEMISPAN.
C  PSPAN    =FRACTION OF WING SEMISPAN.
C  ROOT     =WING ROOT CHORD.
C  DNXS     =SCW (SEE REF. 15), DESIRED NUMBER OF SLOPES (CHORDWISE HORSE-
C            SHOE VOTICES) TO BE USED AT A SPAN STATION.
C  DYS      =VIC (SEE REF. 15), DESIRED NUMBER OF SPAN STATIONS AT WHICH
C            CHORDWISE HORSESHOE VORTICES WILL BE LOCATED.
C  CONST    =INCREMENTAL DISTANCE IN X-COORDINATES FOR SLOPE CALCULATIONS.
C  FUNIM1   =Z-COORDINATE ALONG THE MEAN CAMBER LINE JUST BEFORE EACH CONTROL
C            POINT.
C  FUNIP1   =Z-COORDINATE ALONG THE MEAN CAMBER LINE JUST AFTER EACH CONTROL
C            POINT.
C                    ----------
C  THE FOLLOWING PARAMETERS ASSOCIATE WITH THE LIBRARY SUBROUTINE (STIUNI)
C  USED TWICE IN THIS PROGRAM. THE FIRST, INTERPOLATES THE SLOPES AT THE
C  CONTROL POINT OF EACH GRIDE LINE. THE SECOND, INTERPOLATES THE SLOPES
C  AT THE CONTROL POINT OF EACH ELEMENTAL PANEL FROM THE SLOPES OBTAINED
C  EARLIER.
C  N1, N2   =INPUT INTEGER SPECIFYING THE NUMBER OF NODES.
C  M1, M2   =INPUT INTEGER SPECIFYING THE NUMBER OF STATIONS TO BE INTERPOLATED.
```

```
C  M1, M2  =INPUT INTEGER SPECIFYING THE NUMBER OF STATIONS TO BE INTERPOLATED.
C  XUNI     =INPUT REAL ARRAY OF LENGTH N1 CONTAINING THE X-COORDINATE OF
C           THE NODES. (NONDIMENSIONLIZED WITH LOCAL CHORD.)
C  ZUNI     =INPUT REAL ARRAY OF LENGTH N1 CONTAINING THE Z-COORDINATE OF
C           THE NODES. (NONDIMENSIONLIZED WITH LOCAL CHORD.)
C  TUNI     =INPUT REAL ARRAY OF LENGTH M1 CONTAINING THE X-COORDINATE
C           (OF THE CONTROL POINTS) FOR WHICH INTERPOLATED VALUES OF
C           THE Z-COORDINATE ARE DESIRED.
C  SIGMA    =IT IS A REAL NUMBER, CONTAINING THE TENSION FACTOR. SIGMA
C           INDICATES THE CURVINESS DESIRED FOR INTERPOLATION. ZERO SIGMA
C           PRODUCES AN EXACT CUBIC SPLINE FIT, WHILE IF SIGMA IS FIFTY
C           THE RESULTING CURVE IS PIECEWISE LINEAR.
C  IENDSW   =INPUT INTEGER SPECIFYING THE CONDITION ON THE CURVE AT THE
C           TWO END POINTS. IENDSW=2 CORRESPONDS TO Y"=0.0 .
C  END      =DUMMY VARIABLE, NOT USED IN THIS PROGRAM.
C  IW       =INPUT/OUTPUT INTEGER.
C  FUNI     =OUTPUT ARRAY OF LENGTH M1 CONTAINING THE VALUES OF THE
C           INTERPOLATED Z-COORDINATES CORRESPONDING TO TUNIX. (I.E. TUNIX,
C           FUNI ARE THE X, AND Z COORDINATES OF THE CONTROL POINTS ALONG
C           THE MEAN CAMBER LINE OF DIFFERENT WING SECTION, RESPECTIVELY.)
C  WKU      =INPUT/OUTPUT WORK REAL ARRAY OF LENGTH 2N1-1.
C  IERR     =OUTPUT INTEGER ERROR CODE. ZERO IERR CORRESPONDS TO NORMAL RETURN.
C  XCPT     =LOCAL SLOPES IN CHORDWISE DIRECTION.
C  YCPT     =Y-COORDINATE OF THE CONTROL POINT LOCATIONS ALONG THE MEAN
C           CAMBER SURFACE AT WHICH THE SLOPES ARE DESIRED.
C  LSLOPE   =LOCAL SLOPES IN SPANWISE DIRECTION ALONG THE GRIDE LINES, STARTING
C           FROM LE TO TE AND PROCEEDING FROM INBOARD TO OUTBOARD.
C  FSLOP    =LOCAL SLOPES IN CHORDWISE DIRECTION AT THE CONTROL POINT OF
C           EACH ELEMENTAL PANEL, STARTING FROM INBOARD TO OUTBOARD AND
C           PROCEEDING FROM LE TO TE.
C                    ----------
C  SLSLOP   =LOCAL SLOPES IN CHORDWISE DIRECTION ALONG THE GRIDE LINES,
C           STARTING FROM INBOARD TO OUTBOARD AND PROCEEDING FROM LE TO TE.
C  SLOPCP   =THE SAME AS ABOVE FSLOP.
C  SLOPES   =LOCAL SLOPES IN SPANWISE DIRECTION AT THE CONTROL POINT OF EACH
C           ELEMENTAL PANEL, STARTING FROM LE TO TE AND PROCEEDING FROM
C           INBOARD TO OUTBOARD.
C  ALPHAL   =LOCAL ANGLES OF ATTACK (SLOPES) AT THE CONTROL POINTS IN RADIAN.
C                    ==========
C
      PROGRAM LALPHA (INPUT,OUTPUT,TAPE5,TAPE6,TAPE10)
     REAL XT(16,60),Y(16,69),ZT(16,60),XB(16,60),ZB(16,60),
     1Z(16,60),ZMCAM(16,60),LCHORD(16,60),CHORD(16,1),PSPAN(16)
     1,END(2),FUNI(14),TUNIX(14),WKU(119),XUNI(60),YUNI(60),
     1CONST(2),FUNIM1(16,14),FUNIP1(16,14),WKU2(31),SLOPES(24,14),
     1LSLOPE(16,14),SLSLOP(14,16),XCPT(16),YCPT(24),ALPHAL(24,14),
     1FSLOP(24),SLOPCP(14,24)
      INTEGER IENDSW(2),DNXS,DYS
      REWIND 10
      DATA NS/16/,NODE/60/,ROOT/25.33700/,J1ST/1/,SPAN/16.14760/
      DATA N1/60/,M1/14/,IENDSW/2,2/,SIGMA/30./,DNXS/14/,DYS/24/
      DATA CONST/-0.002,0.002/,N2/16/,M2/24/,CHORDNO/14./
      DATA YCPT/0.02933,0.07865,0.11433,0.15000,0.19000,0.23000,
     1.27500,.32000,.36000,.40000,.44000,.48000,.52500,.57000,
     1.61000,.65000,.69000,.73000,.77863,.82727,.86727,.90363,
     1.94000,.98000/
      DO  10  I  =1,NS
```

```
      DO  10  I  =1,NS
      DO  10  J  =1,NODE
      READ(5,*)XT(I,J),Y(I,J),ZT(I,J)
 10   CHORD(I,1)  =IROOT-XT(I,1)
      DO  11  I=1,NS
      DO  11  J=1,NODE
      READ(5,*)XB(I,J),Y(I,J),ZB(I,J)
 11   PSPAN(I)=Y(I,1)/SPAN
      NODEM1=NODE-1
      DO  13  I=1,NS
      Z(I,1)=ZB(I,1)
      ZMCAM(I,1)=Z(I,1)
      LCHORD(I,1)=0.
      DO  12  J=2,NODEM1
      JM1=J-1
      Z(I,J)=((XT(I,J)-XB(I,JM1))*(ZB(I,J)-ZB(I,JM1)))
     1/(XB(I,J)-XB(I,JM1))+ZB(I,JM1)
      ZMCAM(I,J)=(Z(I,J)+ZT(I,J))/2.
      LCHORD(I,J)=(XT(I,J)-XT(I,1))/CHORD(I,1)
 12   CONTINUE
      LCHORD(I,NODE)=1.
      Z(I,NODE)=ZB(I,NODE)
      ZMCAM(I,NODE)=ZB(I,NODE)
13    CONTINUE
      IW=0
      DO  14  I=1,NS
      DO 100  K=1,2
      DO  15  J=1,NODE
      IF(K.EQ.2) GO TO 17
      XUNI(J)=LCHORD(I,J)
      YUNI(J)=ZMCAM(I,J)/CHORD(I,1)
 17   IF(J.GT.DNXS)GO TO 15
      TUNIX(J)=(FLOAT(J)-0.25)/CHORDNO+CONST(K)
 15   CONTINUE
      CALL STIUNI(N1,M1,XUNI,YUNI,TUNIX,SIGMA,IENDSW,END,IW,FUNI,WKU,
     1IERR)
      IF(IERR.NE.0) GO TO 21
      IF(K.EQ.1)GO TO 111
      IF(K.EQ.2) GO TO 112
 111  DO  118  J=1,DNXS
      FUNIM1(I,J)=FUNI(J)
110   CONTINUE
      GO  TO  100
112   DO  120  J=1,DNXS
      FUNIP1(I,J)=FUNI(J)
120   CONTINUE
 100  CONTINUE
      DO  200  J=1,DNXS
      LSLOPE(I,J)=(FUNIP1(I,J)-FUNIM1(I,J))/(2*0.002)
 200  CONTINUE
 14   CONTINUE
      DO  101  J=1,DNXS
      DO  101  I=1,NS
      SLSLOP(J,I)=LSLOPE(I,J)
 101  CONTINUE
      IW=0
      DO  102  J=1,DNXS
```

```
      DO  102  J=1,DNXS
      DO  103  I=1,NS
      XCPT(I)=SLSLOP(J,I)
103   CONTINUE
      CALL STIUNI(N2,M2,PSPAN,XCPT,YCPT,SIGMA,IENDSW,END,IW,
     1FSLOP,WKU2,IERR)
      IF(IERR.NE.0) GO TO 21
      DO 105 I=1,DYS
      SLOPCP(J,I)=FSLOP(I)
105   CONTINUE
102   CONTINUE
      DO 300 I=1,DYS
      DO 300  J=1,DNXS
      SLOPES(I,J)=SLOPCP(J,I)
      ALPHAL(I,J)=-ATAN(SLOPES(I,J))
300   CONTINUE
C  THE FOLLOWING DO LOOP IS MERELY USED TO REWRITE THE DETERMINED SLOPES
C  IN THE ORDER WHICH VLM-SA CODE REQUIRES.
      DO 600 I=1,DYS
      K=DYS+1-I
      WRITE(10,2)(ALPHAL(K,J),J=1,DNXS)
600   CONTINUE
 2    FORMAT(7F10.6)
      REWIND  10
 21   STOP
      END
```

```
C  ****************************************************************
C  * THE PREVIOUS PROGRAM (I.E. LALPHA) WAS MODIFIED TO GENE-     *
C  * RATE ONLY THE LOCAL ANGLES OF ATTACK ON DIFFERENT LEE         *
C  * GEOMETRIES AS REQUIRED BY THE VLM-SA CODE.  THIS PROGRAM     *
C  * IS SUMMERIZED IN THE FOLLOWING TWO STEPS.                     *
C  * I) DETERMINING THE SLOPES ALONG EACH SPAN STATION.            *
C  * II) INTERPOLATING TO DETERMINE THE DESIRED NUMBER OF          *
C  * SLOPES AT THE CONTROL PIONT OF EACH ELEMENTAL PANEL ON         *
C  * THE LEE SURFACE.                                              *
C  ****************************************************************
C              --------LIST OF VARIABLES---------
C  XLE, Y, ZLE =X, Y, Z-COORDINATE OF THE LEE SURFACE.
C  NONZLE       =NONDIMENSIONLIZED Z-COORDINATE WITH LOCAL CHORD.
C  LECORD       =FRACTION OF LOCAL CHORD. (NONDIMENSIONLIZED WITH LOCAL CHORD)
C  LECORD       =LOCAL CHORD.
C  PLSPAN       =FRACTION OF LOCAL SPAN. (NONDIMENSIONLIZED WITH WING SEMISPAN)
C               ------------------------------------
C  <<<<< COMMENTS FOR THE REMAINING VARIABLE ARE GIVEN IN THE PREVIOUS >>>>>
C                       <<<<<PROGRAM.>>>>>
C
      PROGRAM LEESLP (INPUT,OUTPUT,TAPE5,TAPE10)
      REAL XLE(14,13),Y(14,13),ZLE(14,13),NONZLE(14,13),
     1PLCORD(14,13),LECORD(14),PLSPAN(14)
     1,END(2),FUNI(7),SIGMA,TUNIX(7),WKU(213),XUNI(13),YUNI(13),
     1CONST(2),FUNIM1(14,7),FUNIP1(14,7),WKU2(23),SLOPES(21,7),
     1LSLOPE(14,7),CLSLOP(7,14),XCPT(14),YCPT(21),ALPHAL(21,7),
     1FSLOP(21),SLOPCP(7,21)
      INTEGER IENDSW(2),DNDS,DYS
      DATA NS/14/,NODE/13/,SPAN/16.14700/
      DATA N1/13/,M1/7/,IENDSW/2,2/,SIGMA/50./,DNDS/7/,DYS/21/
      DATA CONST/-0.002,0.002/,N2/14/,M2/21/,CHORDNO/7./
      DATA YCPT/0.02333,0.07855,0.11433,0.15000,0.19000,0.23000,
     1.27500,.32000,.36000,.40000,.44000,.48000,.52500,.57000,
     1.61000,.65000,.69000,.73000,.77863,.82727,.88727/
      DO  10  I=1,NS
      DO  10  J=1,NODE
   10 READ(5,*)XLE(I,J),Y(I,J),ZLE(I,J)
      DO  12  I=1,NS
      PLSPAN(I)=Y(I,1)/SPAN
      DO  11  J=1,NODE
      LECORD(I)=XLE(I,NODE)-XLE(I,1)
      PLCORD(I,J)=(XLE(I,J)-XLE(I,1))/LECORD(I)
      NONZLE(I,J)=ZLE(I,J)/LECORD(I)
   11 CONTINUE
   12 CONTINUE
      IW=0
      DO  14  I=1,NS
      DO 100  K=1,2
      DO  15  J=1,NODE
      IF(K.EQ.2) GO TO 17
      XUNI(J)=PLCORD(I,J)
      YUNI(J)=NONZLE(I,J)
   15 CONTINUE
   17 DO 16 M=1,7
      TUNIX(M)=(FLOAT(M)-0.25)/(CHORDNO)+CONST(K)
   16 CONTINUE
      CALL STIUNI(N1,M1,XUNI,YUNI,TUNIX,SIGMA,IENDSW,END,IW,FUNI,WKU,
```

```
      CALL STIUNI(N1,M1,XUNI,YUNI,TUNIX,SIGMA,IENDSW,END,IW,FUNI,WKU,
     1IERR)
      IF(IERR.NE.0) GO TO 21
      IF(K.EQ.1)GO TO 111
      IF(K.EQ.2) GO TO 112
  111 DO  110  J=1,DNXS
      FUNIM1(I,J)=FUNI(J)
  110 CONTINUE
      GO  TO  100
  112 DO  120  J=1,DNXS
      FUNIP1(I,J)=FUNI(J)
  120 CONTINUE
  100 CONTINUE
      DO  200  J=1,DNXS
      LSLOPE(I,J)=(FUNIP1(I,J)-FUNIM1(I,J))/(2*.002)
  200 CONTINUE
   14 CONTINUE
      DO  101  J=1,DNXS
      DO  101  I=1,NS
      CLSLOP(J,I)=LSLOPE(I,J)
  101 CONTINUE
      IW=0
      DO  102  J=1,DNXS
      DO  103  I=1,NS
      XCPT(I)=CLSLOP(J,I)
  103 CONTINUE
      CALL STIUNI(N2,M2,PLSPAN,XCPT,YCPT,SIGMA,IENDSW,END,IW,
     1FSLOP,WKU2,IERR)
      IF(IERR.NE.0) GO TO 21
      DO 105 I=1,DYS
      SLOPCP(J,I)=FSLOP(I)
  105 CONTINUE
  102 CONTINUE
      DO 300 I=1,DYS
      DO 300  J=1,DNXS
      SLOPES(I,J)=SLOPCP(J,I)
      ALPHAL(I,J)=-ATAN(SLOPES(I,J))
  300 CONTINUE
      DO 600 I=1,DYS
      K=DYS+1-I
      WRITE(10,2)(ALPHAL(K,J),J=1,DNXS)
  600 CONTINUE
    2 FORMAT(7F10.4)
      REWIND  10
   21 STOP
      END
```

B.3 Evaluation

As a part of the present study, it was important to examine the analytical capability of the VLM-SA code for thick wing configuration with leading-edge extensions. For this purpose, the experimental data obtained by Wilson and Lovell, on the thick DM-1 with and without leading edge extension, was selected for validating the results obtained from the VLM-SA code. Although the effect of leading-edge radii is included in the resulting VLM-SA solutions, the thick DM-1, which is a symmetrical wing configuration with 0015-64 NACA airfoil section and no twist, is approximated by its projected planform (flat DM-1) in this analytical study. Experimental lift data obtained by Wilson and Lovell on the DM-1 with and without the leading-edge extension, as well as, the resulting VLM-SA for the same configurations are shown in Fig. B.2. Obviously, the code solutions over-estimate the lift for both the DM-1 and DM-1 + LEE combination throughout the angle of attack range. However, as shown in Fig. B.3, the drag polar comparison shows that, in case of the DM-1, the VLM-SA solutions agree well with experimental data up to lift coefficient of about 0.6. Beyond this lift coefficient, the experimental data tends to deviate from the code's solution, because, as was reported by Wilson and Lovell, the flow over the basic DM-1 appears to become disorganized and result in an increase in drag and a decrease in lift. As a result, the drag polar curve associated with experimental data is higher than the estimated VLM-SA solution. In the case of the DM-1 + LEE combination, the VLM-SA over estimates the drag in the lift

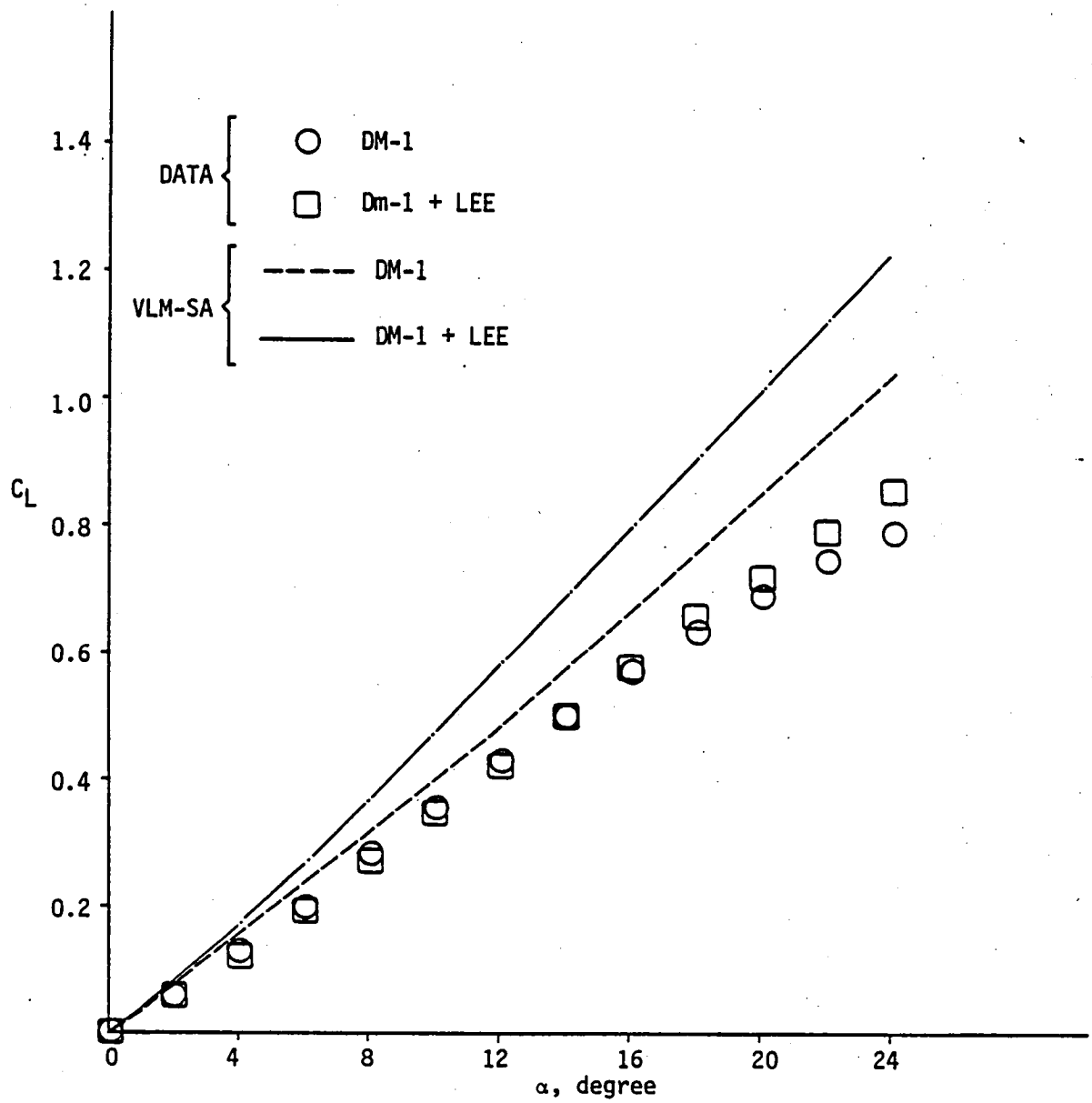

Fig. B.2 Theoretical and experimental lift characteristics.

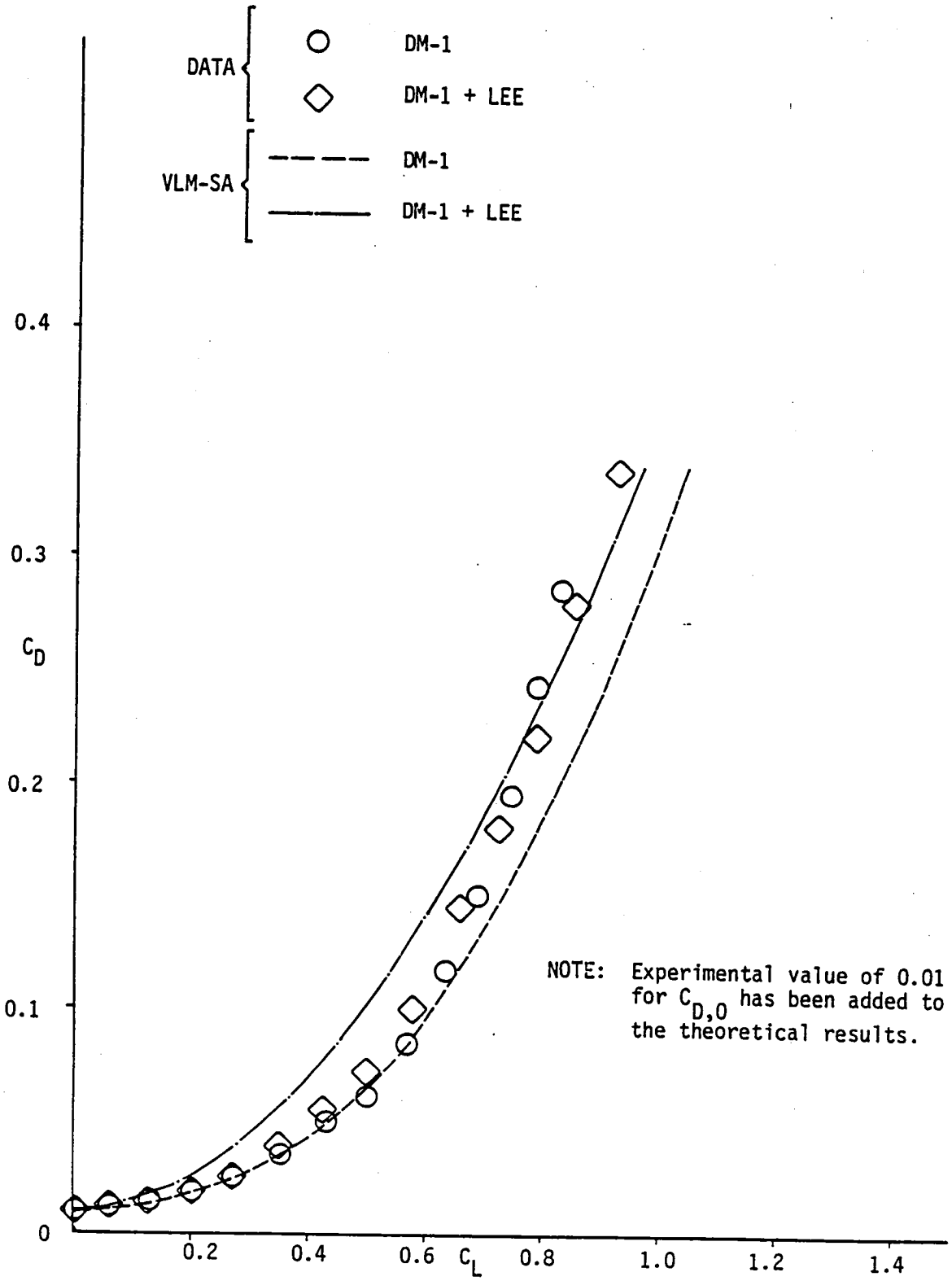

Fig. B.3 Theoretical and experimental drag polars.

coefficient range of about 0.05 to 0.80. This difference was rather expected, because the resulting VLM-SA solutions do not include the effect of the low pressures acting between the LEE and upper surface maximum thickness line of the wing section to produce a thrust. Hence, the computed C_D values are higher than the experimental data. This effect can be seen in Fig. B.4, where lift-to-drag ratio is plotted against lift coefficient. This figure shows again a fair agreement between the code solution and the experimental data up to lift coefficient of about 0.6, for the basic DM-1. However, the L/D theoretical curve associated with the DM-1 + LEE combination is considerably lower than the data points, because of higher drag estimation (note that the lift is also over estimated by the code, Fig. B.2) by the code. Therefore, by analogy it is expected that the VLM-SA solution of drag would be higher in the wing-LEE analysis for the present study.

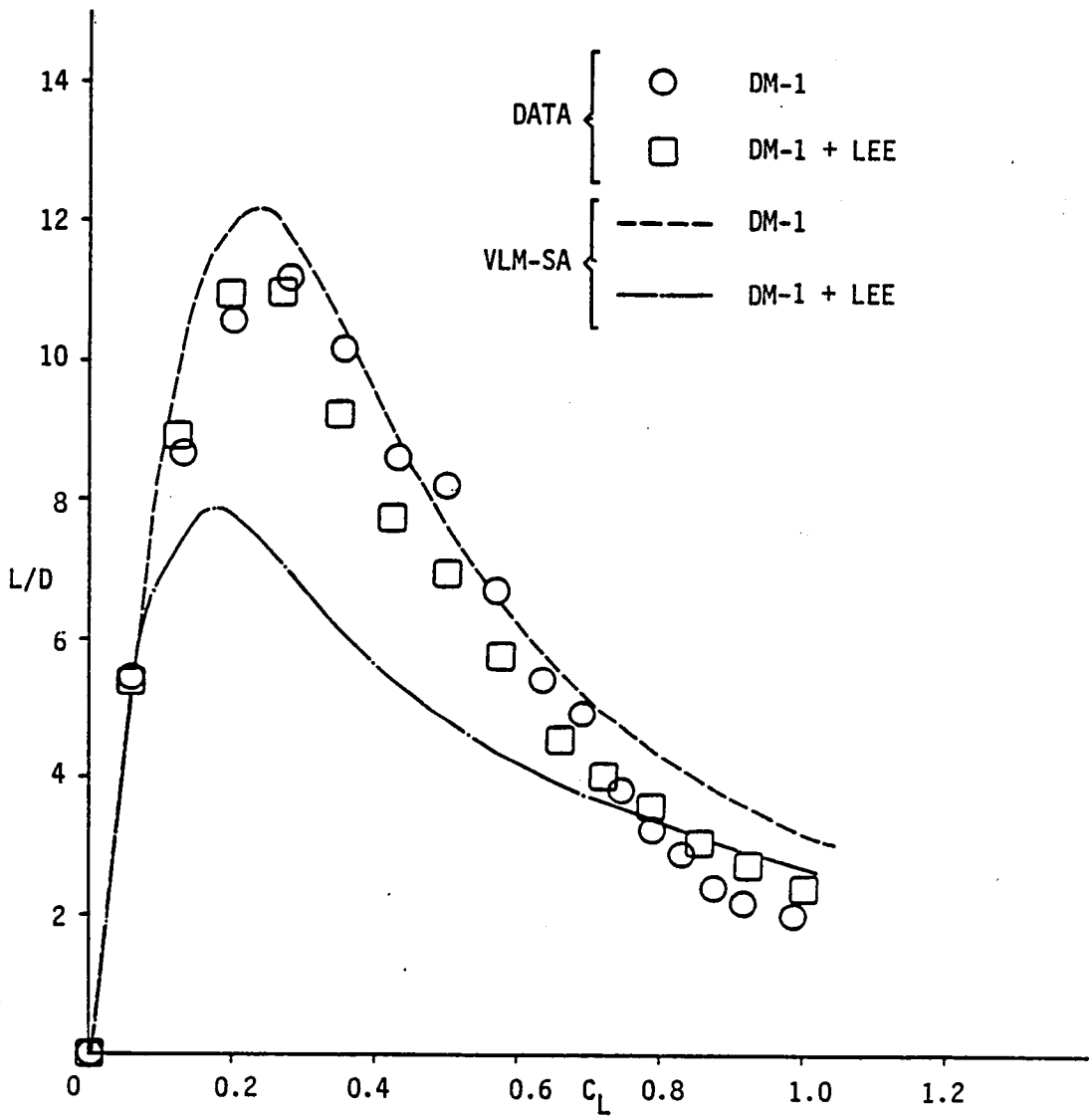

Fig. B.4 Theoretical and experimental lift-to-drag ratios.

1. Report No.	2. Government Accession No.	3. Recipient's Catalog No.
NASA CR-172351		

4. Title and Subtitle	5. Report Date
AN ANALYTICAL DESIGN PROCEDURE FOR THE DETERMINATION OF EFFECTIVE LEADING EDGE EXTENSIONS ON THICK DELTA WINGS	May 1984
	6. Performing Organization Code
7. Author(s)	8. Performing Organization Report No.
Farhad Ghaffari and Sushil K. Chaturvedi	
	10. Work Unit No.
9. Performing Organization Name and Address	11. Contract or Grant No.
Old Dominion University Department of Mechanical Engineering and Mechanics School of Engineering Norfolk, VA	NAS1-17099, Task 26
12. Sponsoring Agency Name and Address	13. Type of Report and Period Covered
National Aeronautics and Space Administration Washington, DC 20546	Contractor Report
	14. Sponsoring Agency Code
	505-31-23-07

15. Supplementary Notes

Langley Technical Monitor: Dr. John E. Lamar

16. Abstract

An analytical design procedure for leading-edge extensions (LEE) has been developed for thick delta wings. This LEE device is designed to be mounted to a wing along the pseudo-stagnation stream surface associated with the attached flow design lift coefficient of greater than zero. The intended purpose of the device is to improve the aerodynamic performance of high subsonic and low supersonic aircraft at incidences above that of attached flow design lift coefficient, by using a vortex system emanating along the leading edges of the device. The low pressure associated with these vortices would act on the LEE upper surface and the forward facing area of the wing leading edges, providing an additional lift and effective leading-edge thrust recovery.

The first application of this technique was to a thick, round-edged, twisted and cambered wing of approximately triangular planform having a sweep of 58° and aspect ratio of 2.3. The panel aerodynamics and vortex lattice methods with suction analogy computer codes were employed to determine the pseudo-stagnation stream surface and an optimized LEE planform shape, respectively.

The aerodynamic effectiveness of 36 different LEE planform shapes was examined for the given wing by considering the influence of geometrical parameters such as chord, sweep angle, and span extent. This investigation showed that the outboard reduction of the LEE span extent minimizes the lift-to-drag ratio, regardless of the LEE's planform shape and area. Also, with the same planform area, it was found that constant chord is relatively more effective than LEE's having sweep angles less than that of the wing.

17. Key Words (Suggested by Author(s))	18. Distribution Statement
Delta wings Thick Vortex flow Transonic	Unclassified - Unlimited Subject Category 02

19. Security Classif. (of this report)	20. Security Classif. (of this page)	21. No. of Pages	22. Price
Unclassified	Unclassified	79	A05